Components Irradiation Test 8

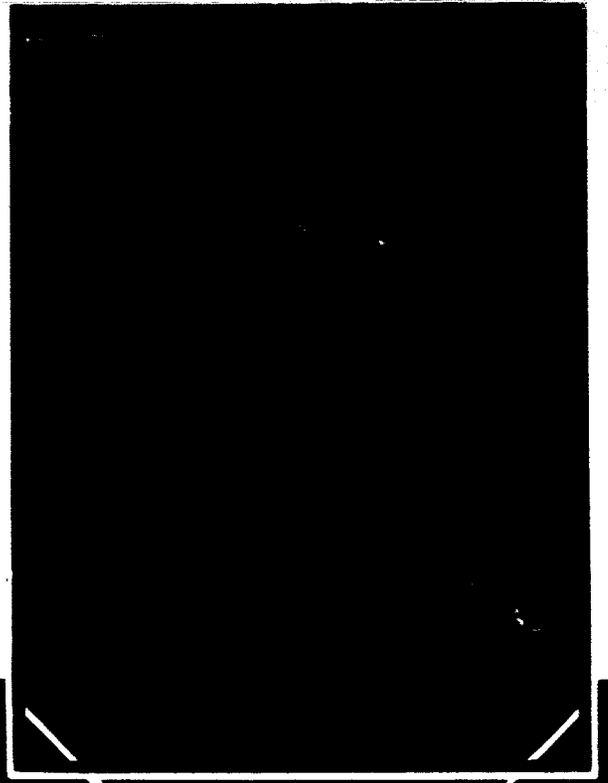

Georgia Nuclear Laboratories
LOCKHEED-GEORGIA COMPANY -- A Division of Lockheed Aircraft Corporation

ER 7686

COMPONENTS IRRADIATION TEST NO. 8
2N918 TRANSISTORS
1N250 DIODES
TANTULUM CAPACITORS

30 OCTOBER 1964

Prepared For:

GEORGE C. MARSHALL SPACE FLIGHT CENTER

Prepared By:

GEORGIA NUCLEAR LABORATORIES

GEORGIA NUCLEAR LABORATORIES
Lockheed-Georgia Company - A Division of Lockheed Aircraft Corporation

If this document is supplied under the requirements of a United States Government contract, the following legend shall apply unless the letter U appears in the coding box:

This data is furnished under a United States Government contract and only those portions hereof which are marked (for example, by circling, underscoring or otherwise) and indicated as being subject to this legend shall not be released outside the Government (except to foreign governments, subject to these same limitations), nor be disclosed, used, or duplicated, for procurement or manufacturing purposes, except as otherwise authorized by contract, without the permission of Lockheed-Georgia Company, A Division of Lockheed Aircraft Corporation, Marietta, Georgia. This legend shall be marked on any reproduction hereon in whole or in part.

The "otherwise marking" and "indicated portions" as used above shall mean this statement and include all details or manufacture contained herein respectively.

Code U	Contract NAS 8-5332

FOREWORD

This report is submitted to the Astrionics Laboratory of the George C. Marshall Space Flight Center, National Aeronautics and Space Administration, Huntsville, Alabama, in accordance with the requirements of Task Order No. ASTR-LGC-18 of Contract No. NAS 8-5332. The report is one of a series describing radiation effects on various electronic components. This particular report concerns transistors, diodes, and capacitors.

The tests were performed by the Georgia Nuclear Laboratories, Lockheed-Georgia Company.

TABLE OF CONTENTS

LIST OF TABLES AND FIGURES

LIST OF TABLES AND FIGURES
(Continued)

Figures

LIST OF TABLES AND FIGURES
(Continued)

Figures Page

1.0 SUMMARY

Forty Fairchild 2N918 transistors, sixty Texas Instruments 2N918 transistors and fifteen Westinghouse 1N250 diodes were subjected to nuclear radiation at a controlled temperature of 46° C. Ten IEI 1000μF capacitors, six Sprague 1000μF capacitors, and six Sprague 140μF capacitors were irradiated in a vacuum environment at ambient temperature. During the irradiation measurements were made to define parameters as follows:

Specimen Type	Parameters
Transistor	h_{FE}, h_{ie}, I_{CBO}
Diode	V_F, I_R
Capacitor	Leakage Current, Capacitance

Test data indicated:

(1) h_{FE} and h_{ie} of the transistors were degraded at about the same rate.

(2) The value of I_C affects the radiation tolerance of the 2N918 transistor.

(3) I_{CBO} values for the 2N918 transistor were on the order of 10^{-8} A and remained so throughout the test.

(4) V_F values for the diodes were increased by irradiation. Different values of I_F had little effect on the rate of increase of V_F.

(5) I_R of the diodes was increased.

(6) Both capacitance and leakage of the capacitors were increased by irradiation. However, both increases appeared to be primarily radiation rate phenomena with no significant permanent change from pre-test values.

(7) All transistors were degraded to less than half their original h_{FE} and all diode specimens increased V_F by more than a factor of two.

2.0 INTRODUCTION

The experiment described in this report is the eighth irradiation of electronic components and is the twelfth in a series of radiation effects tests on electronic equipment, circuits and components contemplated for use on a nuclear space vehicle. Since the use of equipment on this vehicle is contingent upon its ability to withstand the nuclear environment, the Astrionics Laboratory of the Marshall Space Flight Center has undertaken to assure that Government furnished or specified equipment will survive this environment. The equipment is to be subjected to the expected nuclear environment as simulated at the Georgia Nuclear Laboratories. Measurements made on the specimens during the irradiation will describe their radiation tolerance.

The subjects of this test are the 2N918 transistor, the 1N250 diode, a 1000 μF (30 V) capacitor and a 140 μF (75 V) capacitor.

3.0 TEST PROCEDURE

The test specimens were supplied by the Astrionics Laboratory of the Marshall Space Flight Center. During the test the semiconductor specimens were mounted in a controlled temperature chamber held at $46 \pm 2^{\circ}$ C. These specimens were first exposed to a nominal gamma dose of 6.4×10^{5} r behind a neutron attenuator shield. The shielding was then removed and the test was continued until a nominal integrated neutron flux of 7.9×10^{14} n/cm^2 was accumulated. The capacitor specimens were mounted in a vacuum chamber with a nominal vacuum of 10^{-6} Torr during the test, and received a nominal integrated neutron flux of 1.5×10^{14} n/cm^2.

During the first phase of the test an unscheduled reactor shutdown occurred resulting in a short period of zero radiation rate. A complete set of data measurements was not made during this period, but some of the graphs, notably those showing capacitor data, show discontinuities at this point, as well as during the period of reactor shutdown for shield removal.

Before, during and after the irradiation, measurements were made to determine the parameters listed in Table 1. Measurements were also made during the test to define the nuclear, temperature and vacuum environments.

3.1 TEST SPECIMENS

The specimens tested are listed in Table 1. These specimens were mounted by the Astrionics Laboratory. All specimens were new units and had only been subjected to MSFC receiving inspection. Manufacturers' specifications for these specimens are tabulated in Table 2. The specimens were mounted on printed circuit or heat sink boards, which were affixed vertically on the test panel to equalize the radiation flux distribution. Figures 1 through 5 show the relative positions of the

specimens. The test fixtures as shown in Figures 1, 3 and 4 were placed in their respective environmental chambers which were located directly adjacent to the reactor for the irradiation.

3.2 TEST SPECIMEN MEASUREMENTS

A complete set of data was taken prior to reactor startup to establish baseline data for the test. During the irradiation measurements were made at all reactor power settings. Measurements were also made: (a) during reactor shutdown for removal of the shield; (b) immediately after reactor shutdown upon completion of irradiation; (c) approximately ten hours after completion of the irradiation (on non-failed specimens), and 48 hours later for capacitors only. All measurements were performed with the test fixtures in place at the reactor facility.

3.3 INSTRUMENTATION

3.3.1 Transistor Measurement Circuits

The transistor measurement circuits are shown in Figures 6 and 7.. The emitter of each transistor test specimen was commoned, and the base and collector were commutated into the test circuits. In the h_{FE} and the h_{ie} measurement circuit (Figure 7) the feed-back loop, including amplifier "A," establishes the base current necessary to provide a collector current of 10 mA. (See Table 1) Capacitors of 910 pF were connected from collector to emitter of each specimen on the PC boards to prevent oscillations caused by the inductance and capacitance of the long instrumentation cables. These were mica capacitors and had previously shown tolerance well in excess of the radiation levels experienced in this test. The base current was measured by the digital voltmeter and h_{FE} was calculated from these measurements. With a signal current of 10 microamps at 1 kc applied to the base, the base-to-emitter voltage (V_{be}) was measured by an ac voltmeter. These values

were used in determination of the input impedance (h_{ie}). The system accuracy of the I_{CBO} measurement circuit, Figure 6, was $\pm$ 1% $\pm$ 10 nA.

3.3.2 Diode Measurement Circuits

The circuits in Figures 8 and 9 were used to perform the diode measurements with the GNL digital voltmeter data logging system. The cathode of all diodes were commoned and the anodes were commutated into the test circuit. Potential leads for the diode specimens were used to eliminate the voltage drop in the 300 foot instrumentation cables to the test specimens. The maximum sensitivity for reverse current measurements was in the order of 10^{-7} amps. The different forward currents used are shown in Table 1.

3.3.3 Capacitor Measurement Circuits

The capacitor measurement circuits are shown in Figures 10 and 11. Leakage current of the instrumentation cabling without specimens attached was measured separately. These values were subtracted from the total leakage of the system to give the corrected capacitor leakage. The 30 and 75 VDC bias was applied to the 1000 μF and 140 μF capacitors, respectively, five minutes prior to measurement. The system sensitivity of the leakage measurement was 10^{-10} amps. The capacitance was measured using a 60 cycle capacitance bridge with 30 and 75 VDC applied to the specimens during measurement.

3.4 TEST ENVIRONMENT

3.4.1 Pressure

During the test the transistors and diode specimens were at atmospheric pressure while the capacitors were at a vacuum of approximately 10^{-6} Torr. See Figure 12 for vacuum environment during the irradiation test.

3.4.2 Temperature

The transistor and diode specimens were located in an environmental chamber at a temperature of 46 $\pm$ 2° C during the test. Near the end of the test the temperature of these specimens rose to 49 $\pm$ 3° C because of gamma heating. The capacitor specimens were at ambient temperature in the vacuum chamber. See Figure 13 for capacitor temperature environment during the test.

3.4.3 Nuclear

The irradiation was performed in two radiation phases with a lapse of about one hour between phases. For the semiconductor specimens, the first phase was conducted with a lithium hydride shield and 8" water jacket shield interposed between the environmental chamber and the reactor. For the capacitor specimens in the vacuum chamber, the first phase was with a water shield only. The second phase for all specimens was without shielding. The neutron to gamma ratio at the semiconductor specimens was 2.3×10^5 nvt/r, at the capacitor specimens 2.4×10^7 nvt/r, and without shielding, 1.2×10^8 nvt/r at all locations. During the irradiation both neutron and gamma radiations were monitored and recorded.* Isoline radiation flux plots were made for the test panels and used in the data reduction.

* A more detailed description of the GNL Nuclear Measurement System is contained in a previous report; viz. Components Irradiation Test No. 1, ER-6785, Georgia Nuclear Laboratories, Dawsonville, Georgia.

4.0 METHOD OF DATA ANALYSIS

The transistor and diode data were recorded by the GNL Data Logging System. This system recorded parameter measurements in typewritten digital form and simultaneously punched the data in 5-channel perforated tape. A tape-to-card converter was used to transfer the h_{FE}, h_{ie}, I_{CBO}, and V_F data to IBM cards which were then programmed into an IBM 7094 computer to yield h_{FE}, h_{FE_n} (normalized h_{FE}), h_{ie}, h_{ie_n} (normalized h_{ie}), I_{CBO} and V_F. Normalization was accomplished by dividing each parameter value by its corresponding preirradiation value. I_R for the diodes was processed manually. All capacitor parameters were recorded and processed manually.

The mean parameter value for a data group, where shown, was computed by adding the individual specimen parameter values and dividing the sum by the number of specimens.

The median parameter value for a data group (that value which divides a distribution so that an equal number of items is on either side of it) was determined from a plot of the individual specimen parameter values on an arithmetic probability chart. The limits of the 68% envelopes were determined by picking off those values within which were contained 34% of the specimens next above the group median value and 34% of the specimens next below the group median value. The limits of the 95% and 99.7% envelopes were found in a similar fashion. The 7094 computer performed these functions for those parameters which were computer processed. The median and envelope limits for other parameters were determined graphically in the same manner.

In those cases where the parameter of an individual specimen behaved significantly differently from the group median, these "unusual" specimens have been portrayed separately.

For those groups which contained less than 10 specimens the data for each specimen has been shown.

Radiation environmental data shown on the figures' abscissae were obtained by integrating, with respect to time, the gamma dose rates and neutron flux rates.

Those figures which show "Percent Failed Versus Integrated Neutron Flux" were prepared after the procedure described by Mr. Frank W. Poblenz in an article entitled, "Analysis of Transistor Failure in a Nuclear Environment," which appeared in Volume NS-10, Number 1, January 1963, of the IEEE Transactions on Nuclear Science. This type of presentation enables the circuit designer to predict the radiation level at which any given percentage of the particular component will equal or exceed the failure criteria.

Copies of the reduced data from which the graphs were prepared are on file in the Astrionics Laboratory of the Georga C. Marshall Space Flight Center, NASA, Huntsville, Alabama, and in the Georgia Nuclear Laboratories, Lockheed-Georgia Company, Dawsonville, Georgia.

5.0 TEST DATA AND DISCUSSION OF RESULTS

The test data have been presented herein in graphical form. The radiation exposure is, in all cases, a combination of neutrons and gammas. The abscissa scale on each of the graphs is accumulated neutrons/cm^2 greater than 0.5 MeV. However, the coincident accumulated gamma dose (r) is also indicated at those points where changes in the reactor power rate occurred. It is important to remember that the total radiation exposure consists of both neutrons and gammas, and that each may contribute, in varying degrees, to the degradation of a component's parameter.

5.1 TYPE 2N918 TRANSISTOR

5.1.1 The h_{FE} Parameter

h_{FE} was measured at each of two I_C values. Figures 14, 15, 16 and 17 show the results obtained. The dispersion of h_{FE} values about the median was greater at I_C = 3 mA than at I_C = 30 mA; this was true for both manufacturers. All four figures show a discontinuity of slope at the point of shield removal. This indicates that the gamma dose is a significant factor in the degradation of h_{FE}. Figures 18, 19, 20, and 21 show the failure patterns of the specimens under test. Figure 22 is a composite of the four preceding figures to facilitate comparison. From Figure 22 it can be seen that the Texas Instruments specimens at I_C = 3 mA had failures extending over the widest range of radiation exposure. In the case of both manufacturers, specimens performed longer at I_C = 30 mA than at I_C = 3 mA.

Initial values of h_{FE} and orders of failure for each of the manufacturers and test conditions are shown as follows:

Fairchild, I_C = 3 mA

h_{FE_o}	Order of Failure
32.40	30
34.37	18
35.09	16
36.44	10
37.47	19
37.96	22
38.06	24
38.54	27
39.70	5
42.85	12
43.44	7
44.18	13
44.97	28
45.54	25
46.74	35
50.01	17
50.43	6
52.05	21
56.13	29
57.37	34
57.65	23
58.02	14
58.15	31
59.24	2
60.84	9
60.86	8

Fairchild, I_C = 3 mA (Continued)

h_{FE_o}	Order of Failure
61.95	15
62.46	1
63.73	36
68.17	33
70.94	20
72.24	32
72.48	3
73.33	4
93.72	26
103.10	11

These data show no correlation between h_{FE_o} and order of failure.

Fairchild, I_C = 30 mA

h_{FE_o}	Order of Failure
29.27	27
33.48	30
34.64	15
35.89	34
36.14	14
37.83	19
38.27	29
38.86	22
39.01	20
40.60	36

Fairchild, I_C = 30 mA (Continued)

h_{FE_o}	Order of Failure
42.08	35
43.29	23
43.35	32
43.48	10
43.99	31
43.99	25
46.44	18
49.26	21
50.51	26
51.37	4
52.36	8
52.82	33
53.29	17
55.25	11
55.45	5
56.29	13
56.29	28
58.03	24
58.71	12
59.17	7
59.29	16
62.63	3
63.29	6
66.52	2
66.52	9
69.77	1

These data indicate good correlation between high h_{FE_o} and early failure.

Texas Instruments, I_C = 3 mA

h_{FE_o}	Order of Failure
27.08	58
27.13	43
27.26	54
27.47	59
28.22	60
28.82	49
29.70	51
29.99	52
30.05	47
30.18	55
30.34	40
30.82	57
32.24	50
34.37	56
35.38	48
35.85	44
36.87	38
37.40	53
37.48	31
37.96	27
38.31	45
38.43	42
39.85	46
41.06	39
41.72	23
42.66	36

Texas Instruments, I_C = 3 mA (Continued)

h_{FE_o}	Order of Failure
44.10	30
44.19	21
44.39	15
45.74	25
46.22	29
46.81	9
47.55	19
49.64	33
51.20	14
53.29	20
54.29	16
54.48	41
55.67	22
56.24	24
56.53	10
56.83	17
57.70	26
58.95	4
59.50	18
62.12	8
62.12	5
62.46	2
62.46	35
62.91	6
63.79	11
63.95	3
65.16	32

Texas Instruments, I_C = 3 mA (Continued)

h_{FE_o}	Order of Failure
68.79	37
74.61	34
74.93	28
77.94	1
78.93	7
93.49	13
123.00	12

These data show good correlation between high h_{FE_o} and early failure.

Texas Instruments, I_C = 30 mA

h_{FE_o}	Order of Failure
30.55	54
30.93	46
31.45	59
33.63	45
35.55	35
36.32	44
36.50	40
36.76	60
36.90	57
37.04	55
37.88	58
39.32	43
39.84	51

Texas Instruments, I_C = 30 mA (Continued)

h_{FE_o}	Order of Failure
40.71	56
40.87	24
40.93	41
41.38	33
42.02	52
42.13	36
42.25	23
43.35	37
43.86	53
43.99	39
43.99	38
44.31	50
44.38	47
44.44	42
44.64	49
44.71	34
44.78	31
45.80	48
45.87	15
46.01	30
46.66	14
48.86	18
50.42	16
50.59	22
51.37	29
52.36	2

Texas Instruments, I_C = 30 mA (Continued)

h_{FE_o}	Order of Failure
53.57	28
55.25	20
55.35	9
55.45	8
57.36	4
58.14	11
58.48	25
60.00	5
60.61	10
60.73	12
63.16	7
63.29	26
64.38	21
67.87	27
68.03	19
70.75	32
70.92	1
74.63	17
76.53	3
80.00	13
99.01	6

In these data, correlation between high h_{FE_o} and early failure is very good.

5.1.2 The h_{ie} Parameter

Useable h_{ie} data were obtained from about half of the specimens of each group. For the other specimens interference from 60 cycle sources was such that the 60 cycle component was greater than 10% of the 1000 cycle component. For this reason the data was considered not useable. Figures 23 and 24 show the normalized h_{ie} data for each of the two groups. The similarity of these figures to the corresponding figures showing the normalized h_{FE} data (Figures 14 through 17) may be explained by the relationship:

$$h_{ie} = r_{bb} + h_{fe}\, r_e$$

where r_{bb} = base spreading resistance

and r_e = emitter junction resistance

Since $h_{fe} \approx h_{FE}$ the expression may be written

$$h_{ie} \approx r_{bb} + h_{FE}\, r_e$$

Normally $h_{FE}\, r_e$ (or $h_{fe}\, r_e$) is the predominant factor and thus controls h_{ie}.

5.1.3 The I_{CBO} Parameter

Figure 25 shows the I_{CBO} data for the group of Fairchild specimens. The pre-irradiation median value was .026 μA. The median decreased during the first part of the test to near the limit of instrumentation sensitivity (about 10^{-8} A) and remained at this low value throughout the test. There was partial recovery toward pre-irradiation value during the reactor shutdown period for shield removal.

Except for the two unusual specimens shown in Figure 26, the group of Texas Instruments specimens had I_{CBO} values below the limit of instrumentation

sensitivity (10^{-8} A) before, during, and after the irradiation.

5.2 TYPE 1N250 DIODE (WESTINGHOUSE)

5.2.1 The V_F Parameter

V_F was measured at each of three values of I_F, 0.5A, 2.5A, and 5.0A. Figures 27, 28, and 29 show the data for these measurements. Dispersion of values about the median was least for I_F = 0.5A and greatest for V_F = 5.0A. Behavior of V_F during irradiation was similar in all three cases with very little difference in the ranges of radiation exposure over which failures occurred.

Figures 30, 31, and 32 show the failure patterns for the three differenc I_F values. Figure 33 is a composite of the three preceding figures and shows no significant difference existed between the failure patterns.

5.2.2 The I_R Parameter

Figure 34 shows the I_R data measured at V_R of 200V. The data shown have been corrected for instrumentation cable leakage. Two "unusual" specimens which did not reasonably follow the median of the others are shown in the same figure. These "unusual" specimens were not included in determination of the median and envelopes for the group.

5.3 CAPACITORS

5.3.1 Capacitance

The capacitance of the two types (1000μF and 140μF) capacitors was measured at 60 cps. This data was plotted as a function of integrated neutron flux in Figures 35, 36, and 37. The data seem to indicate a slight increase in capacitance at each of the two highest radiation rates. This parameter returns to its approximate

original value when the reactor is shut down, therefore, it seems to be a rate effect. At no time during the irradiation do any of the capacitors exceed their rated tolerance of $\pm$ 20% .

5.3.2 Leakage Current

Leakage current was measured for both types of capacitors with 30 VDC applied to the 1000μF and 75 VDC applied to the 140μF capacitors. This data was plotted versus integrated neutron flux in Figures 38, 39, 40, 41, and 42. The discontinuities on the graphs indicate rapid increases or decreases in leakage when the power level of the reactor was being changed. Since the leakage for all of the specimens returned to the approximate pre-test values when the reactor was shut down, the increases are probably a radiation rate effect. The permanent change was not significant.

TABLE I TEST SPECIMENS AND TEST CONDITIONS

Board No.	Description	No. Tested	Test Conditions	Parameter Measured
1 & 2	Transistor 2N918, NPN, Si Fairchild	40	V_{CB} = 15 V, I_E = 0	I_{CBO}
			V_{CE} = 1V, I_C = 3 mA	h_{FE}
			V_{CE} = 1V, I_C = 30 mA	h_{FE}
			V_{CE} = 1V, I_C = 3 mA I_{sig} = 10 μA at 1 kc	h_{ie}
3, 4 & 5	Transistor 2N918, NPN, Si Texas Instruments	60	V_{CB} = 15 V, I_F = 0	I_{CBO}
			V_{CE} = 1V, I_C = 3 mA	h_{FE}
			V_{CE} = 1V, I_C = 30 mA	h_{FE}
			V_{CE} = 1V, I_C = 3 mA I_{sig} = 10 μA at 1 kc	h_{ie}
6 & 7	Diode 1N250 Westinghouse	15	I_F = .5A	V_F
			I_F = 2.5A	V_F
			I_F = 5.0A	V_F
			V_R = 200 V	I_R
8	Capacitor 1000 μF, 30 V IEI	10	30 VDC	Leakage Current
			30 VDC, 60 cps	Capacitance
9	Capacitor 1000 μF, 30 V Sprague (300D173)	6	30 VDC	Leakage Current
			30 VDC, 60 cps	Capacitance
9	Capacitor 140 μF, 75 V Sprague (200D200)	6	75 VDC	Leakage Current
			75 VDC, 60 cps	Capacitance

TABLE 2 MANUFACTURERS' SPECIFICATIONS OF TEST SPECIMENS

Test Specimens	Conditions	Specifications
Transistor, 2N918 Fairchild Texas Instruments	V_{CB} = 15V, T = 25° C V_{CB} = 15V, T = 150° C V_{CE} = 1V, I_C = 3 mA	I_{CBO} = .010 μA I_{CBO} = 1 μA h_{FE} = 20 Min
Diode, IN250 Westinghouse	I_F = 25A, T = 25° C V_R = 200V, T = 150°	V_F = 1.5V I_R = 5.0 mA
Capacitor, 100 μF Sprague 200D173 IEI (Specifications not known)	Max. 1/2 VAC RMS at 120 cps at 25° C 30 VDC at 125° C	1000 μF ± 20% Max. 105 μA at 25 ± 5° C Max. 510 μA at 85 ± 3° C
Capacitor, 140 μF Sprague, 200D200	Max. 1/2 VAC RMS at 120 CPS at 25° C 75 VDC at 125° C	140 μF ± 20% Max. 36.7 μA at 25 ± 5° C Max. 178 μA at 85 ± 3° C

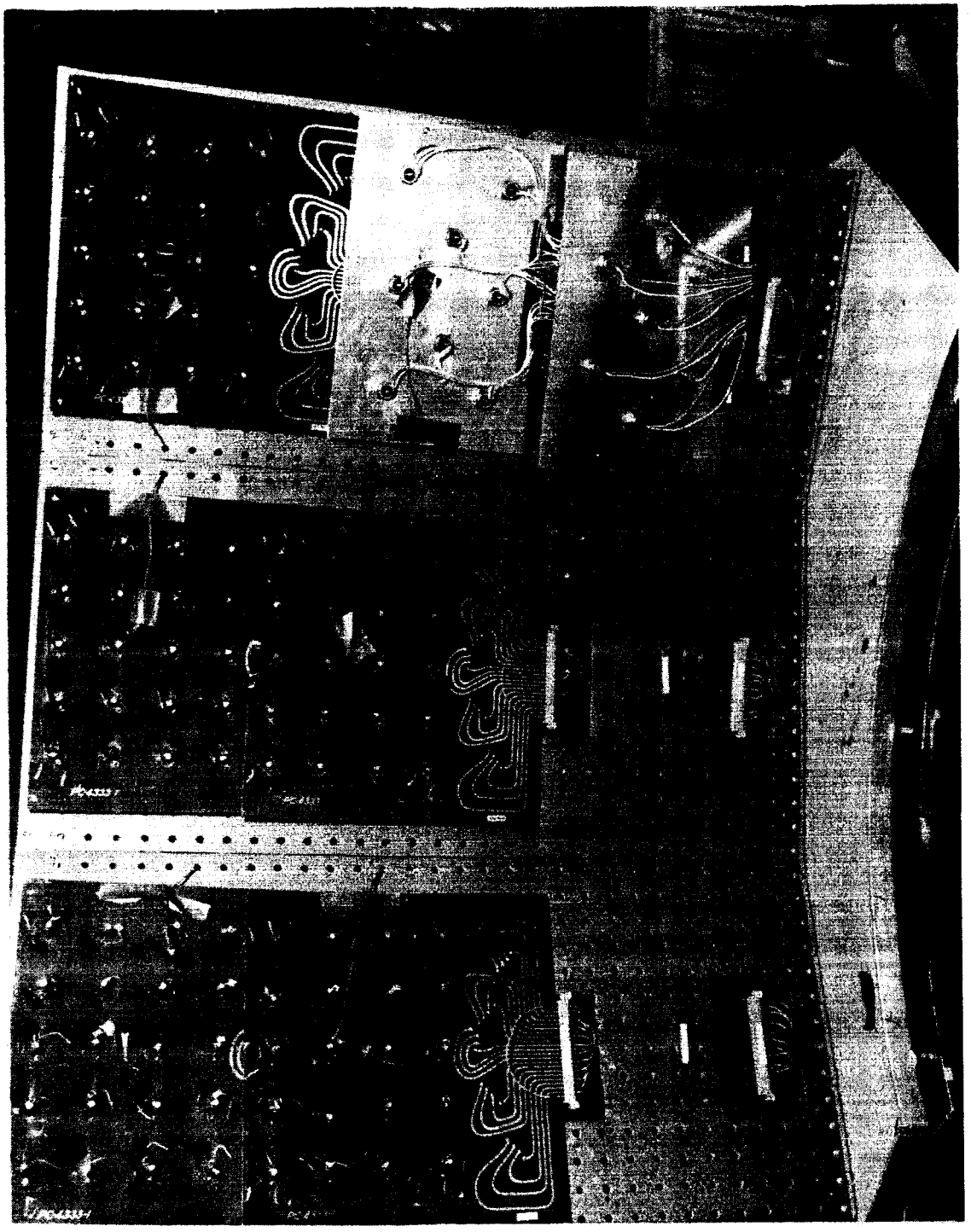

FIGURE 1 TRANSISTOR AND DIODE TEST PANEL

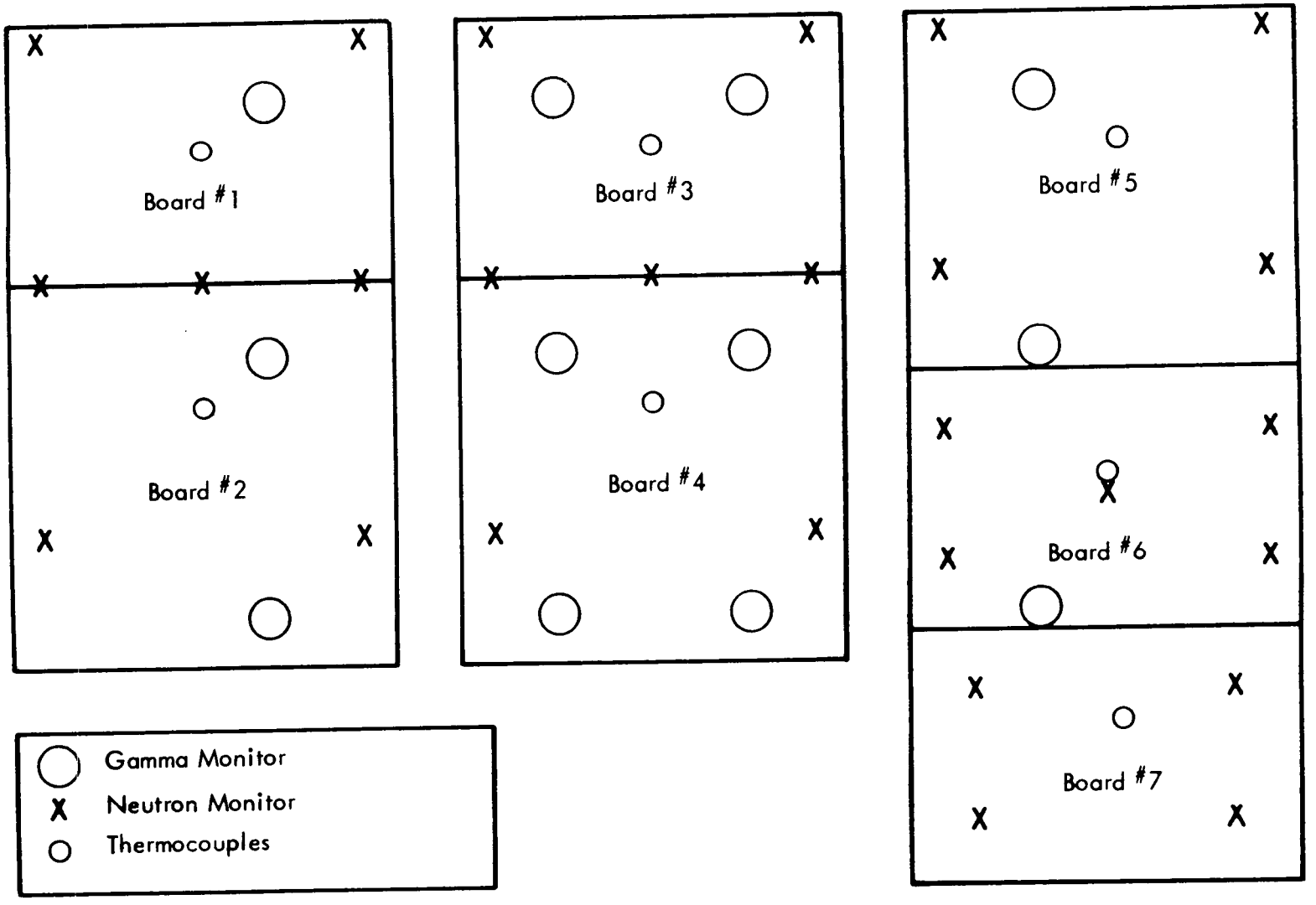

FIGURE 2 DIAGRAM OF TEST PANEL AS SEEN FROM REACTOR

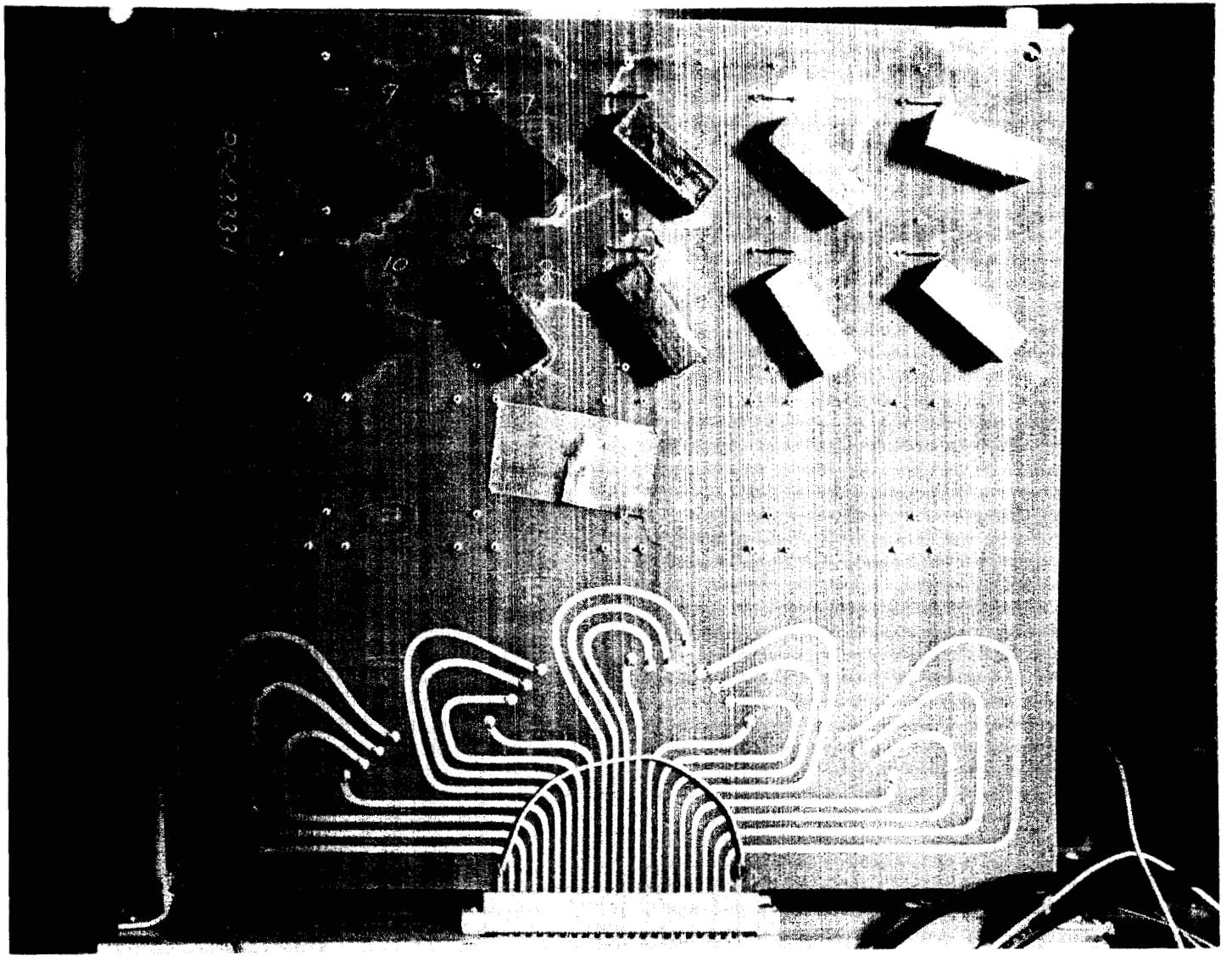

FIGURE 3 CAPACITOR TEST PANEL (FRONT)

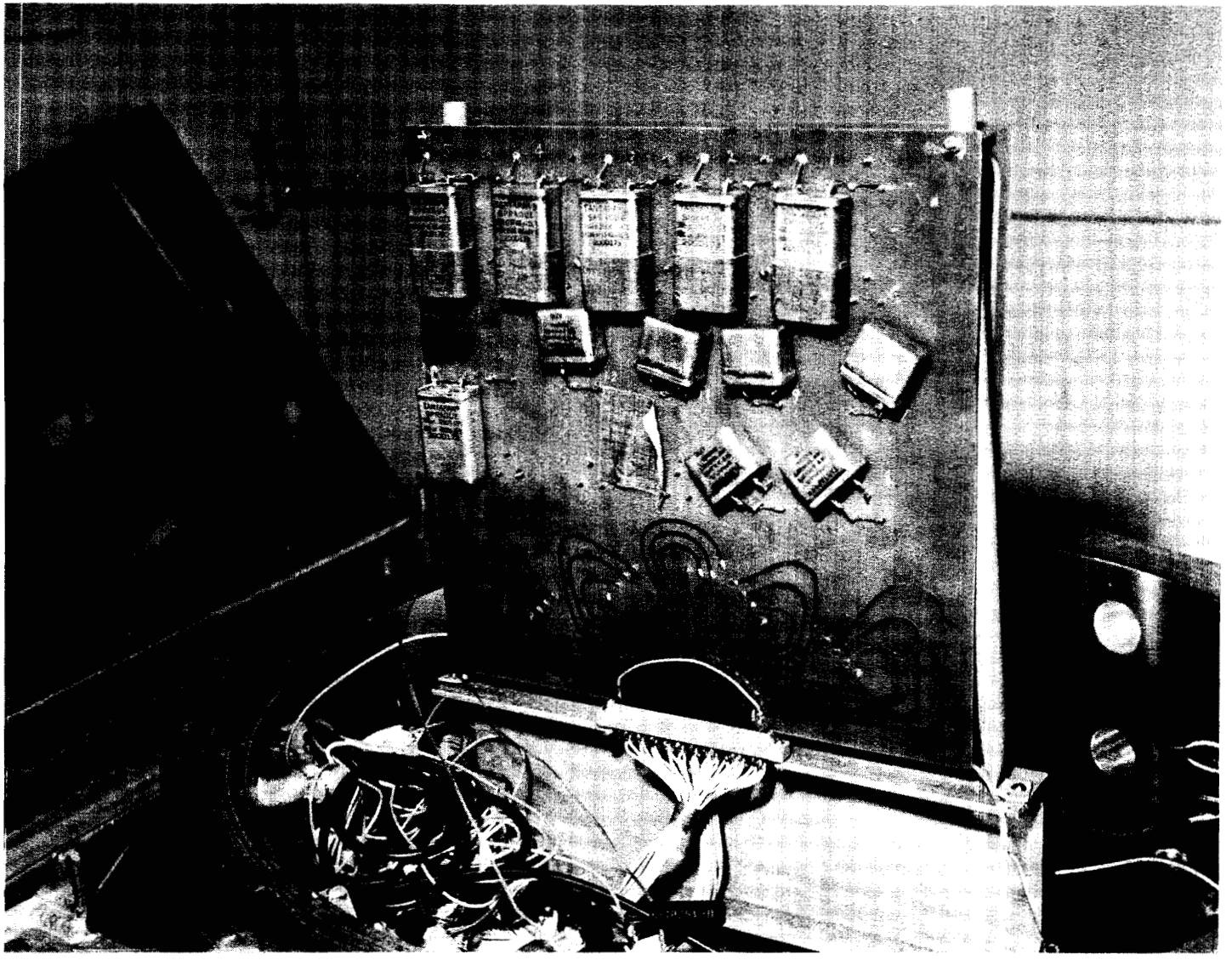

FIGURE 4 CAPACITOR TEST PANEL (REAR)

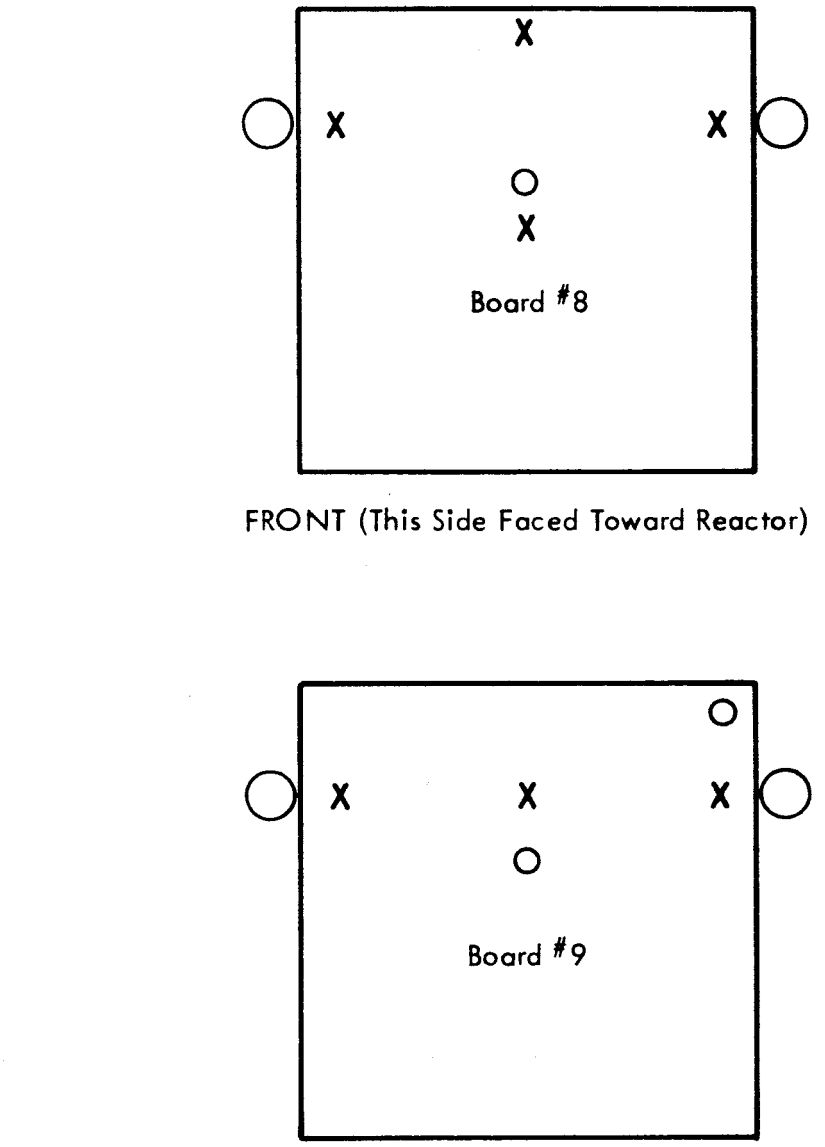

FIGURE 5 DIAGRAM OF CAPACITOR TEST PANEL

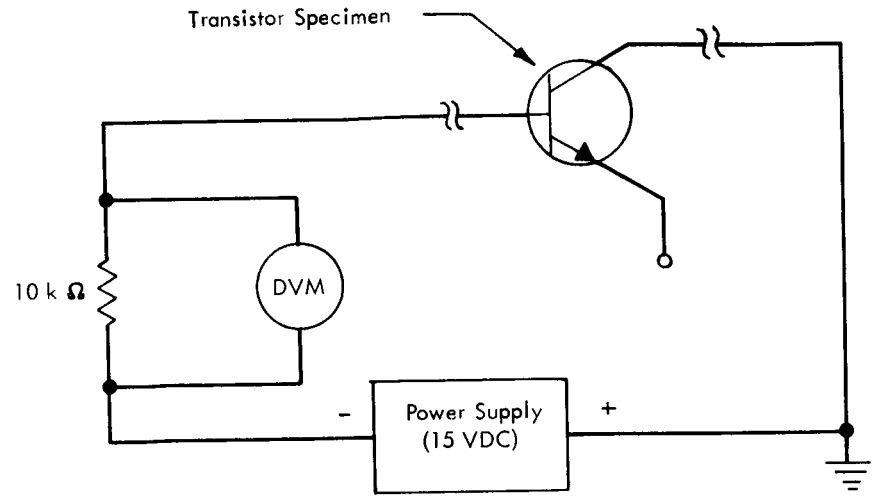

FIGURE 6 I_{CBO} MEASURING CIRCUIT

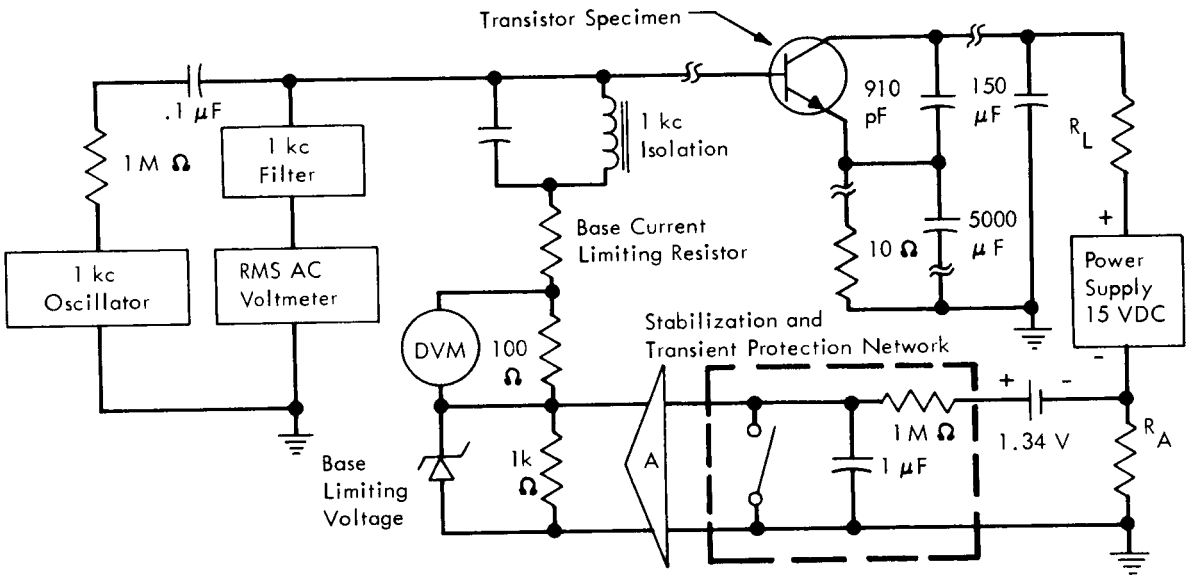

I_C	R_L	R_A
3 mA	4.6 kΩ	447 Ω
30 mA	40 Ω	44.7 Ω

FIGURE 7 h_{FE} AND h_{ie} MEASURING CIRCUIT

I_F	R
0.5 A	106 Ω
2.5 A	20 Ω
5.0 A	9 Ω

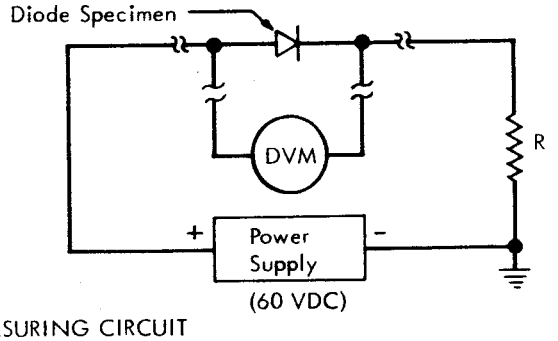

FIGURE 8 V_F MEASURING CIRCUIT

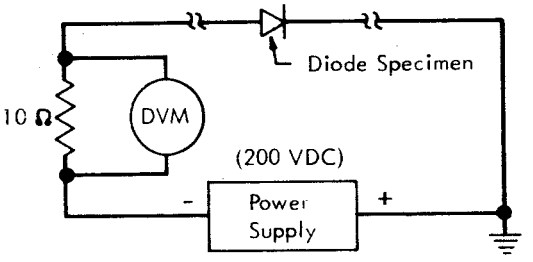

FIGURE 9 I_R MEASURING CIRCUIT

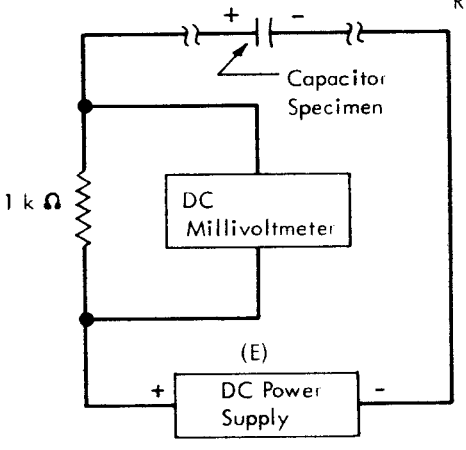

Specimen	E
IEI, 1000 μF	35 VDC
Sprague, 1000 μF	35 VDC
Sprague, 140 μF	75 VDC

FIGURE 10 LEAKAGE CURRENT MEASURING CIRCUIT

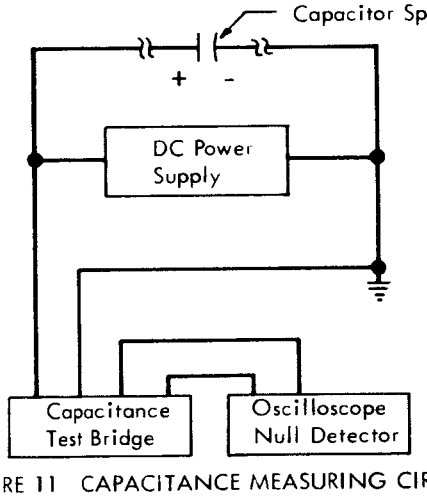

FIGURE 11 CAPACITANCE MEASURING CIRCUIT

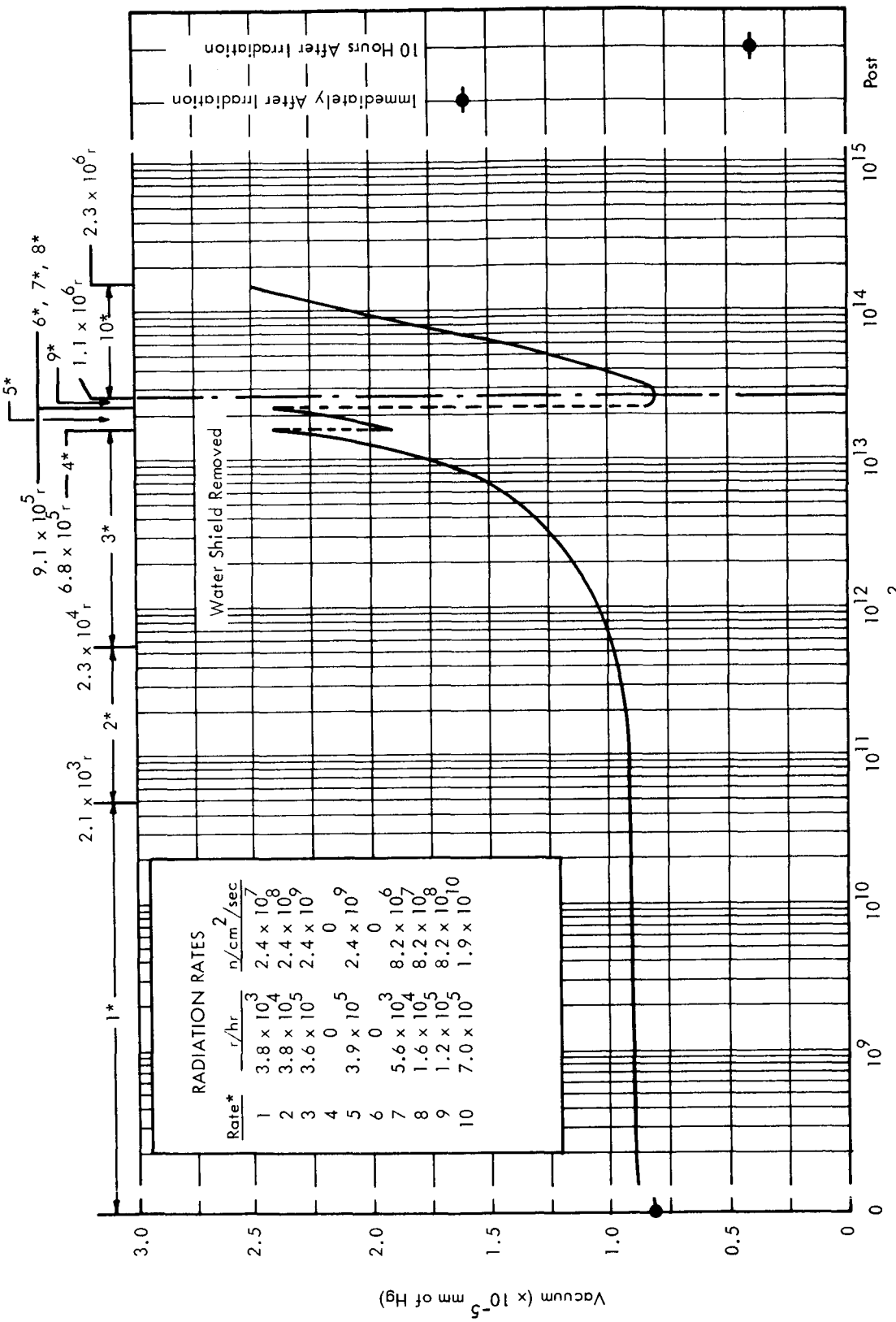

FIGURE 12 VACUUM ENVIRONMENT VERSUS INTEGRATED NEUTRON FLUX

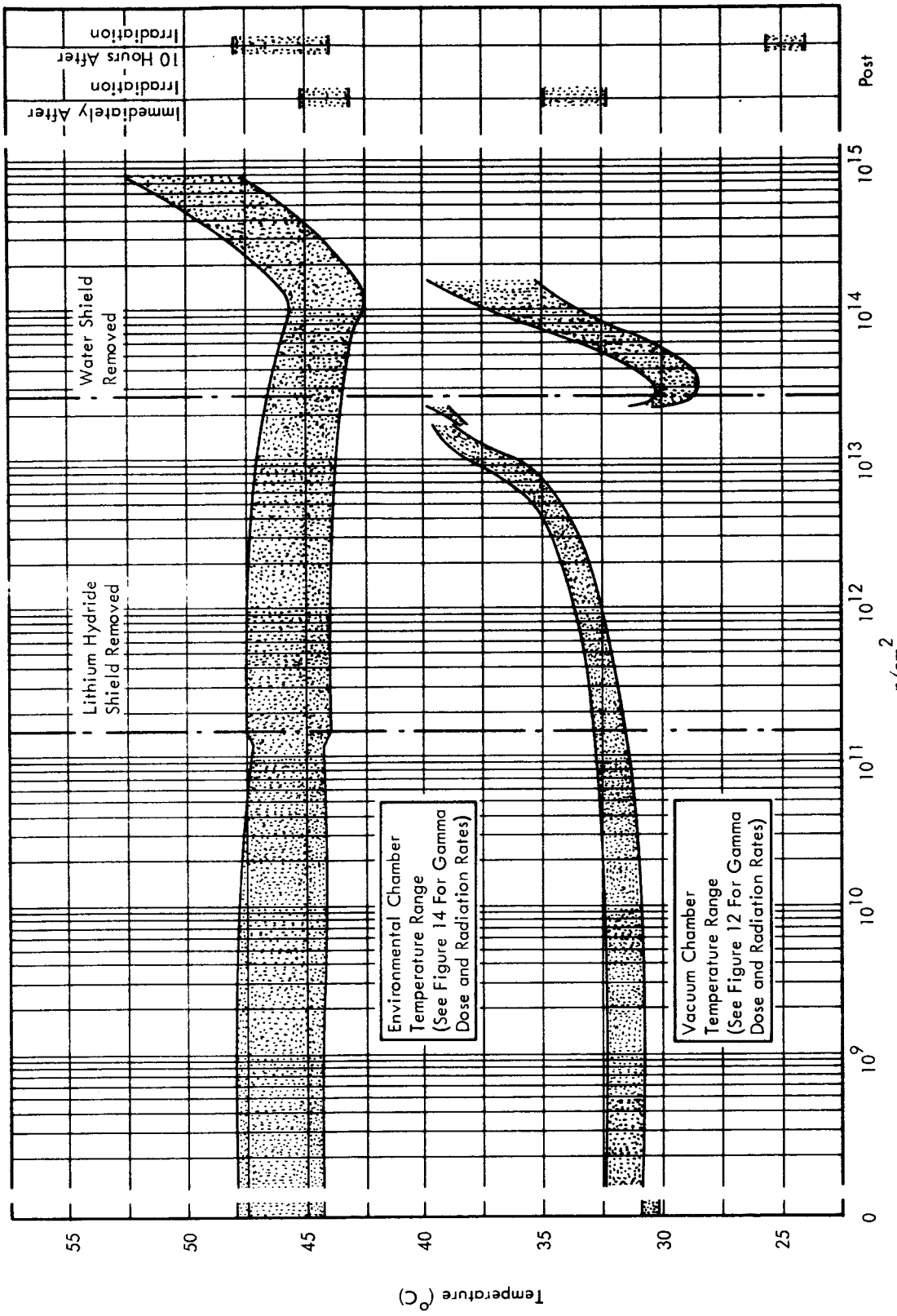

FIGURE 13 TEMPERATURE VERSUS INTEGRATED NEUTRON FLUX

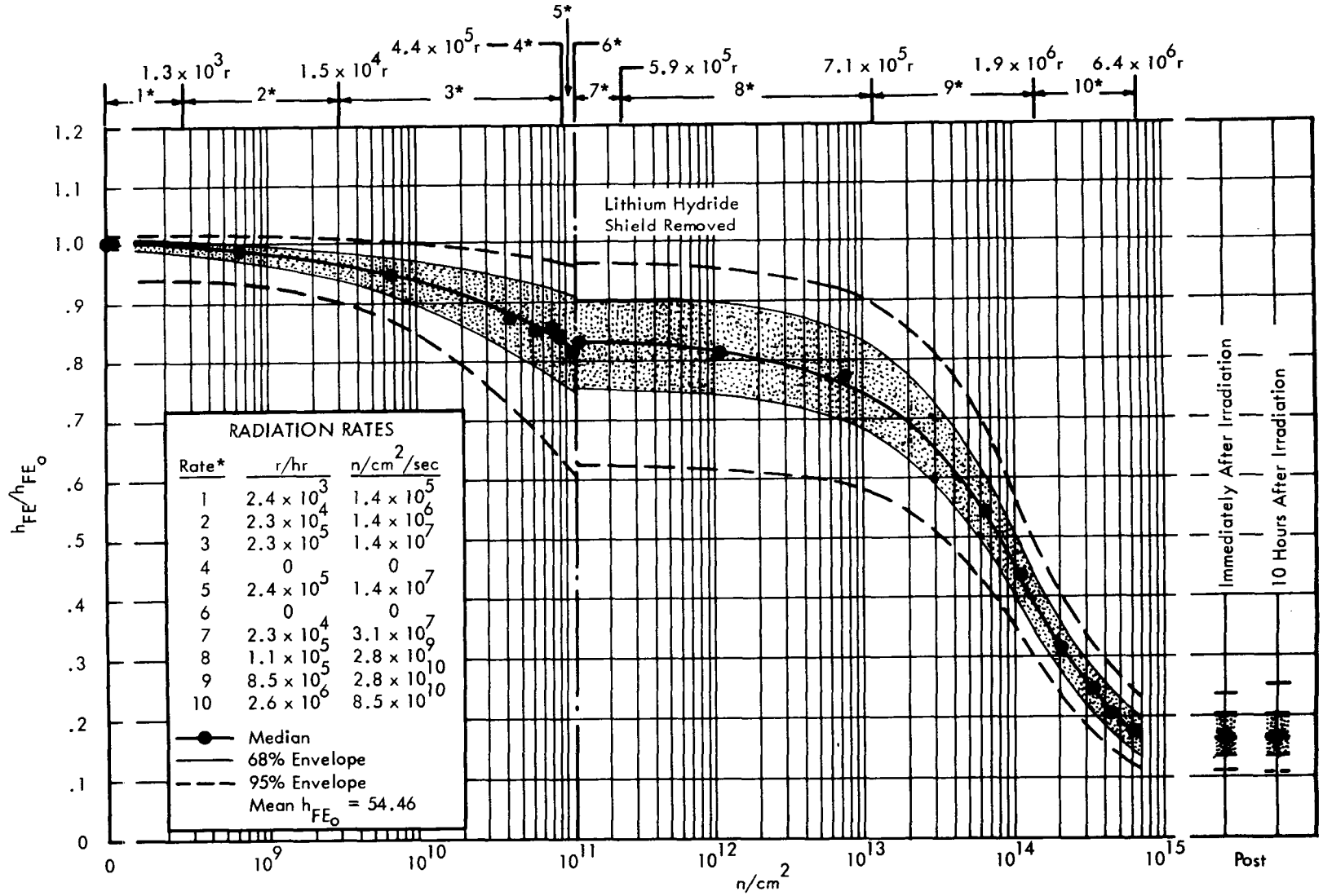

FIGURE 14 2N918 FAIRCHILD, 46° C, NORMALIZED h_{FE} (I_C = 3 mA) VERSUS INTEGRATED NEUTRON FLUX

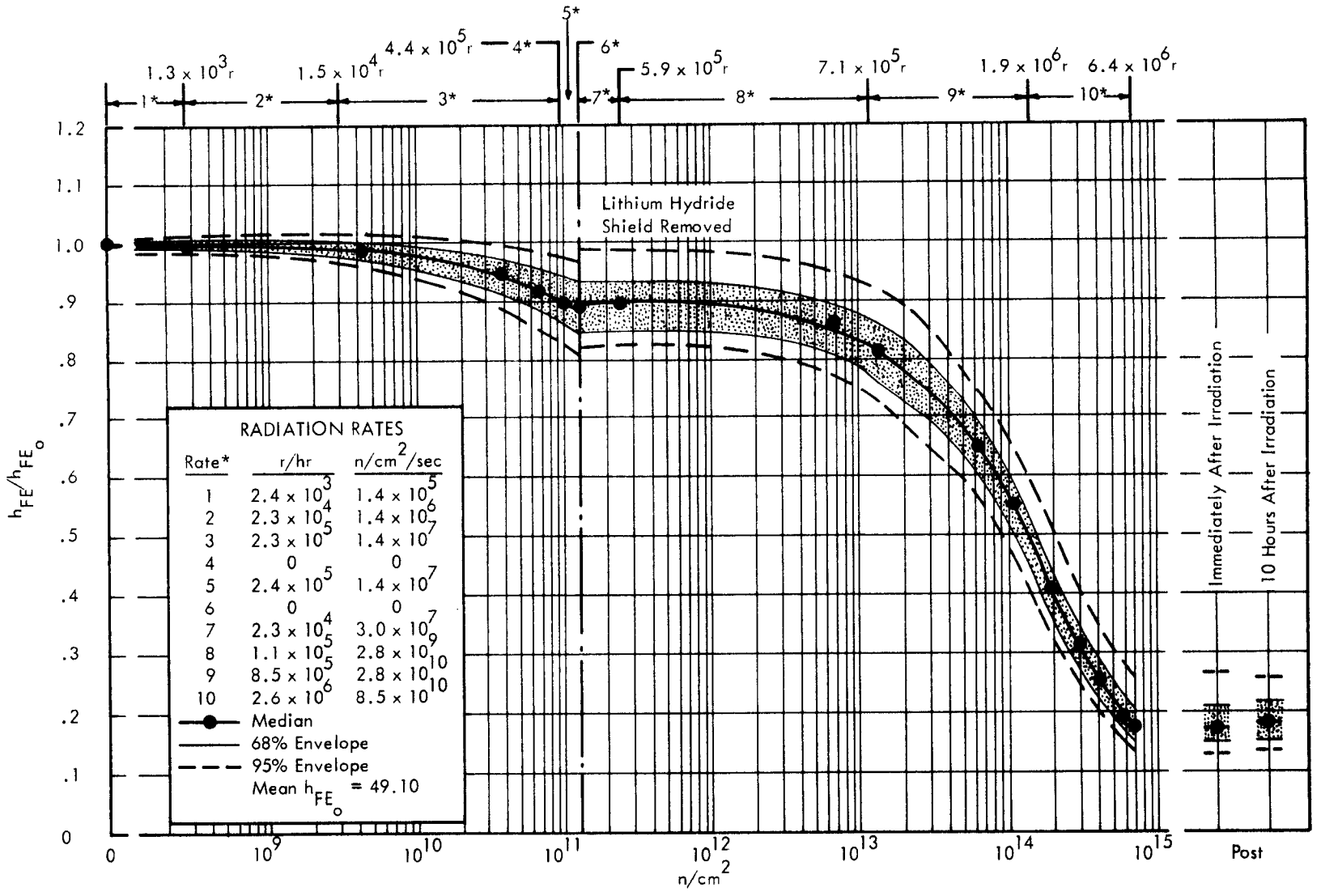

FIGURE 15 2N918 FAIRCHILD, 46° C, NORMALIZED h_{FE} (I_C = 30 mA) VERSUS INTEGRATED NEUTRON FLUX

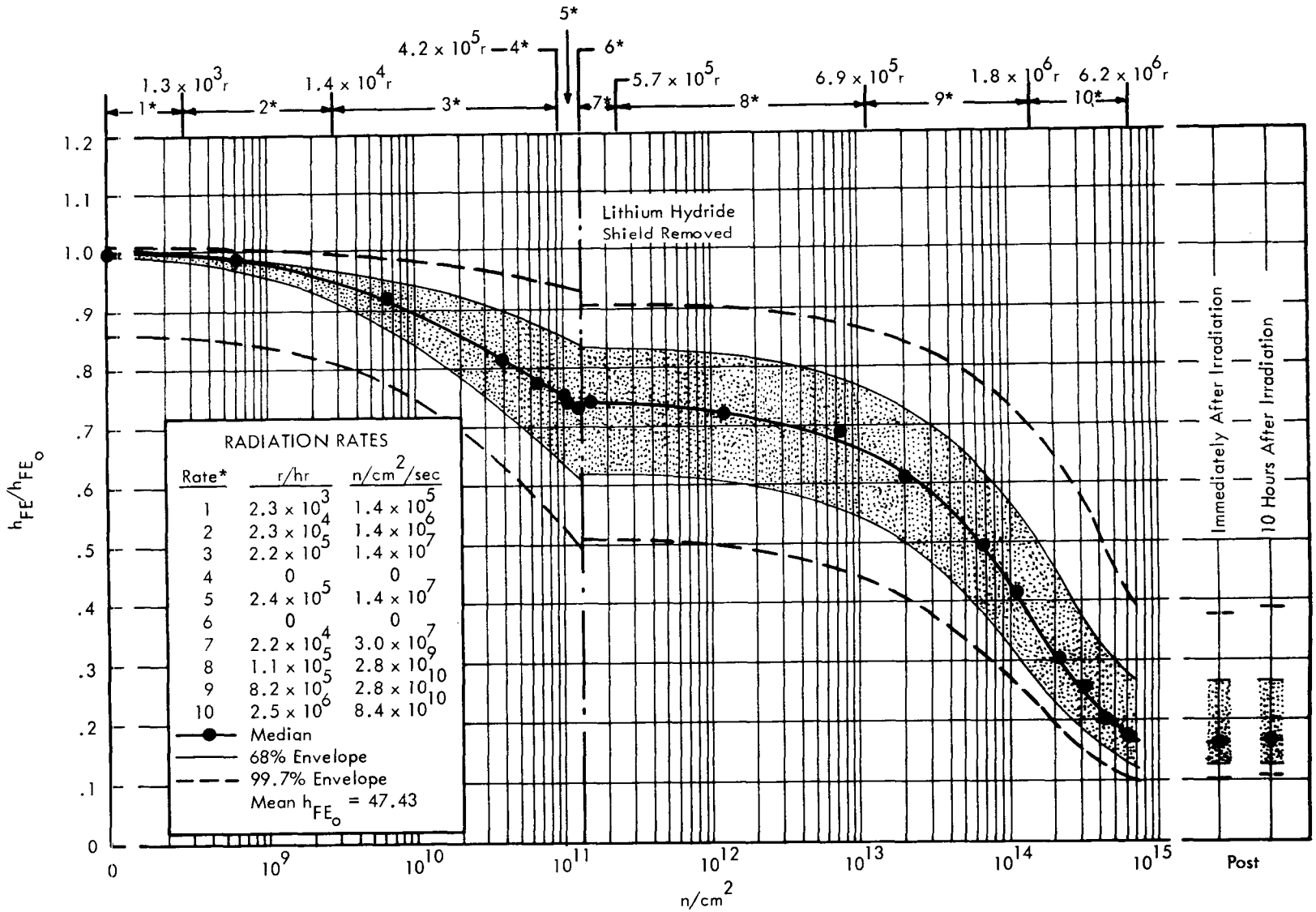

FIGURE 16 2N918 TEXAS INSTRUMENTS, 46° C, NORMALIZED h_{FE} (I_C = 3 mA) VERSUS INTEGRATED NEUTRON FLUX

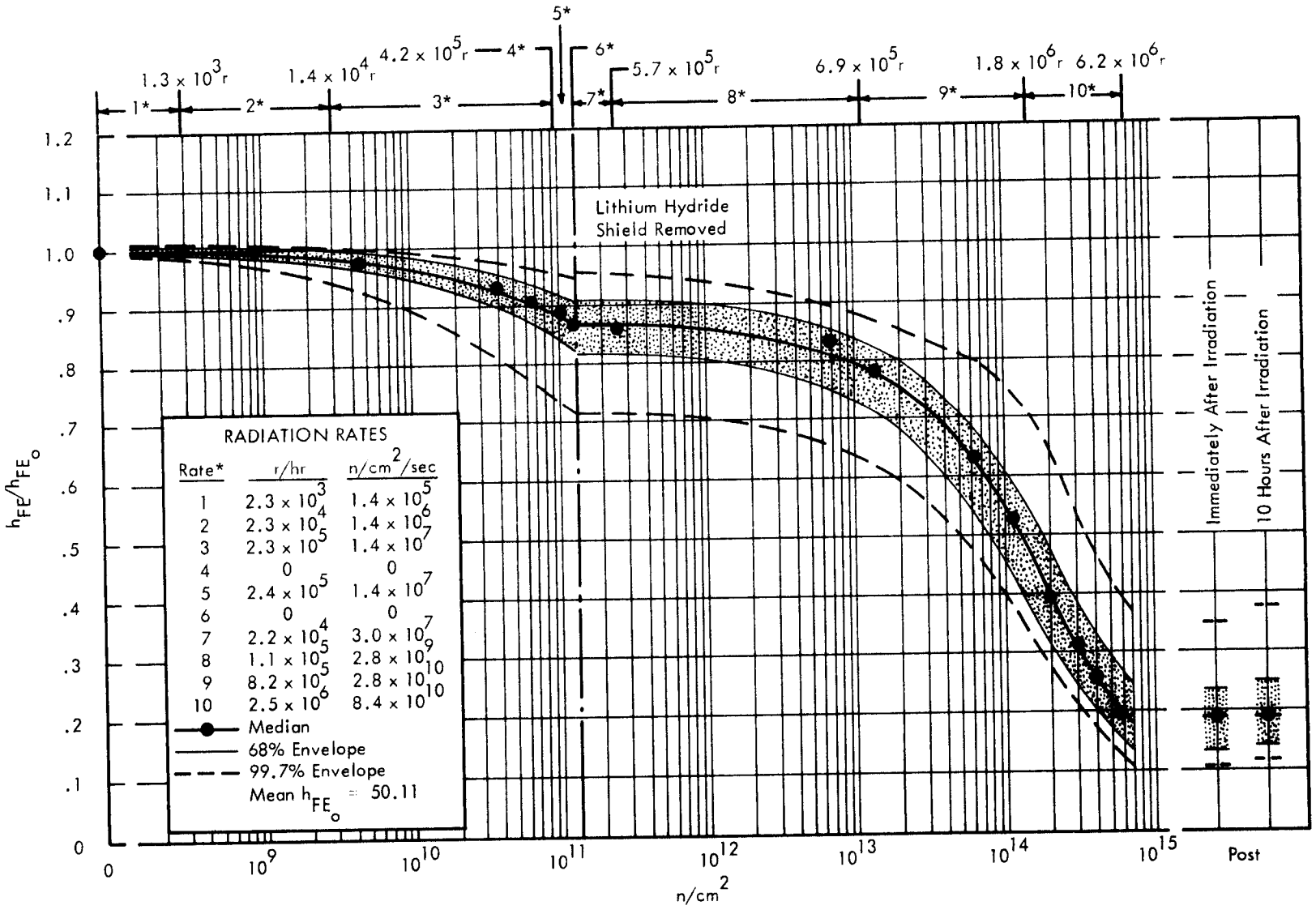

FIGURE 17 2N918 TEXAS INSTRUMENTS, 46° C, NORMALIZED h_{FE} (I_C = 30 mA) VERSUS INTEGRATED NEUTRON FLUX

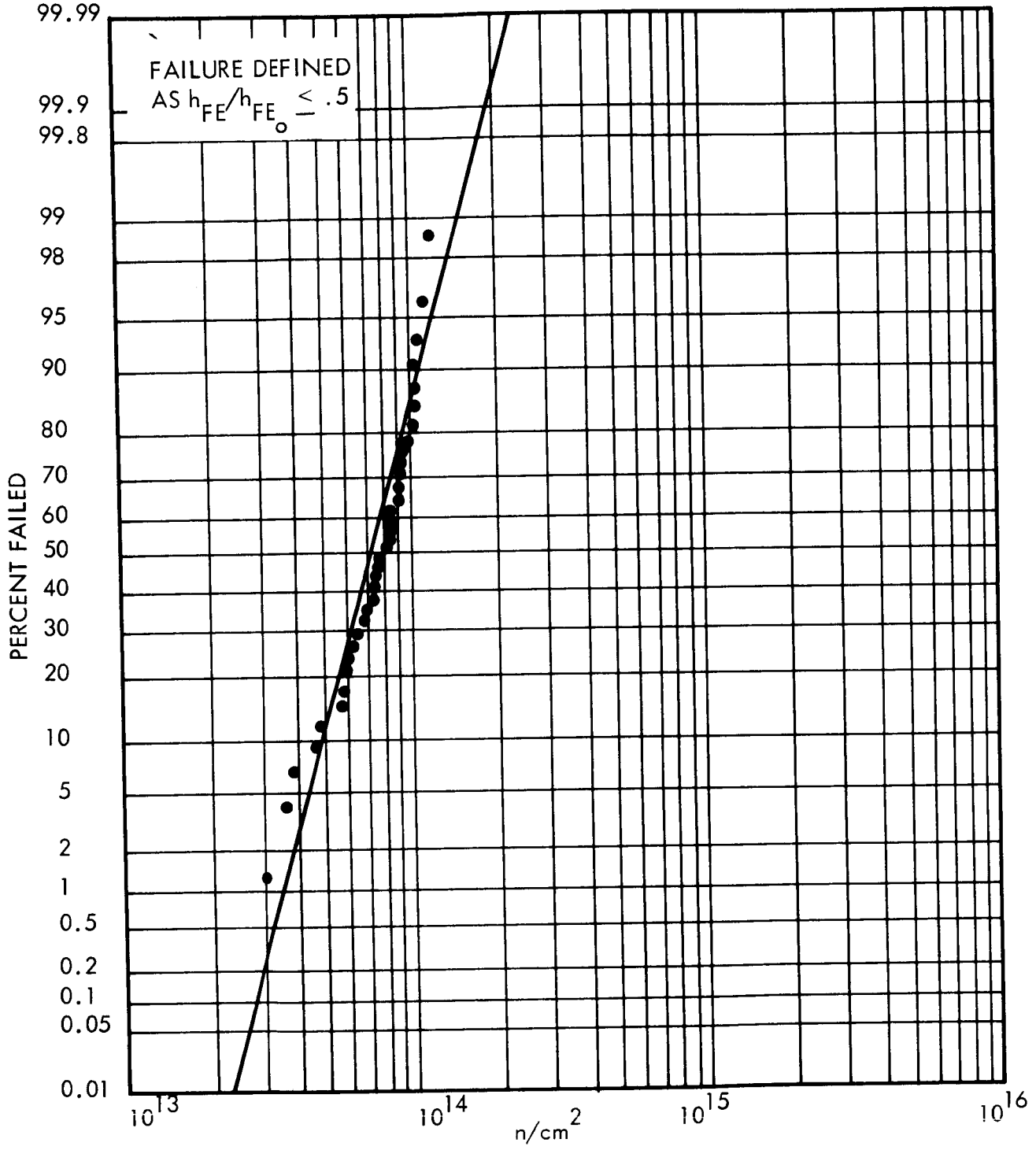

FIGURE 18 2N918, FAIRCHILD, 46°C, (I_C = 3 mA), PERCENT FAILED VERSUS INTEGRATED NEUTRON FLUX

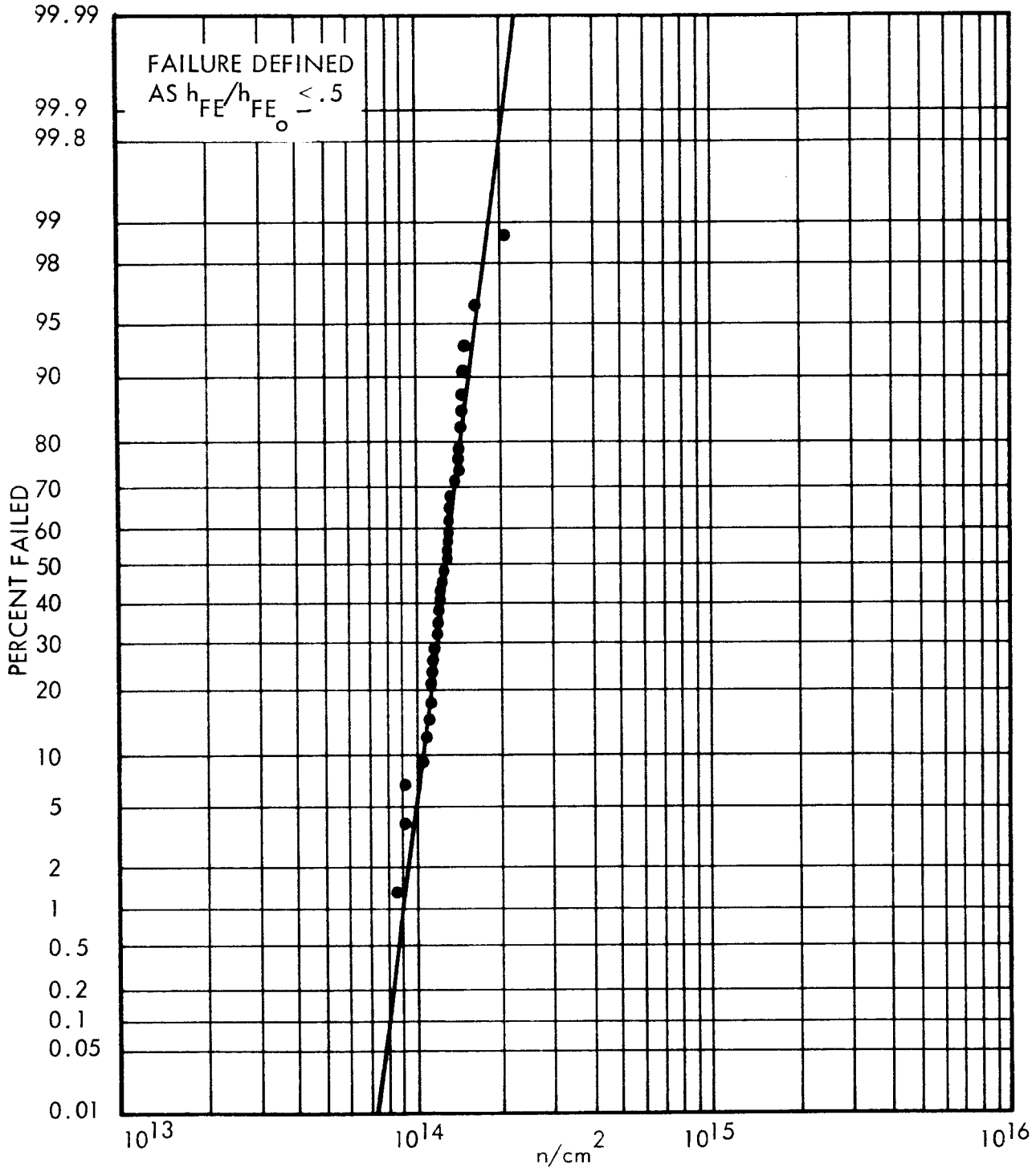

FIGURE 19 2N918 FAIRCHILD, 46°C, (I_C = 30 mA), PERCENT FAILED VERSUS INTEGRATED NEUTRON FLUX

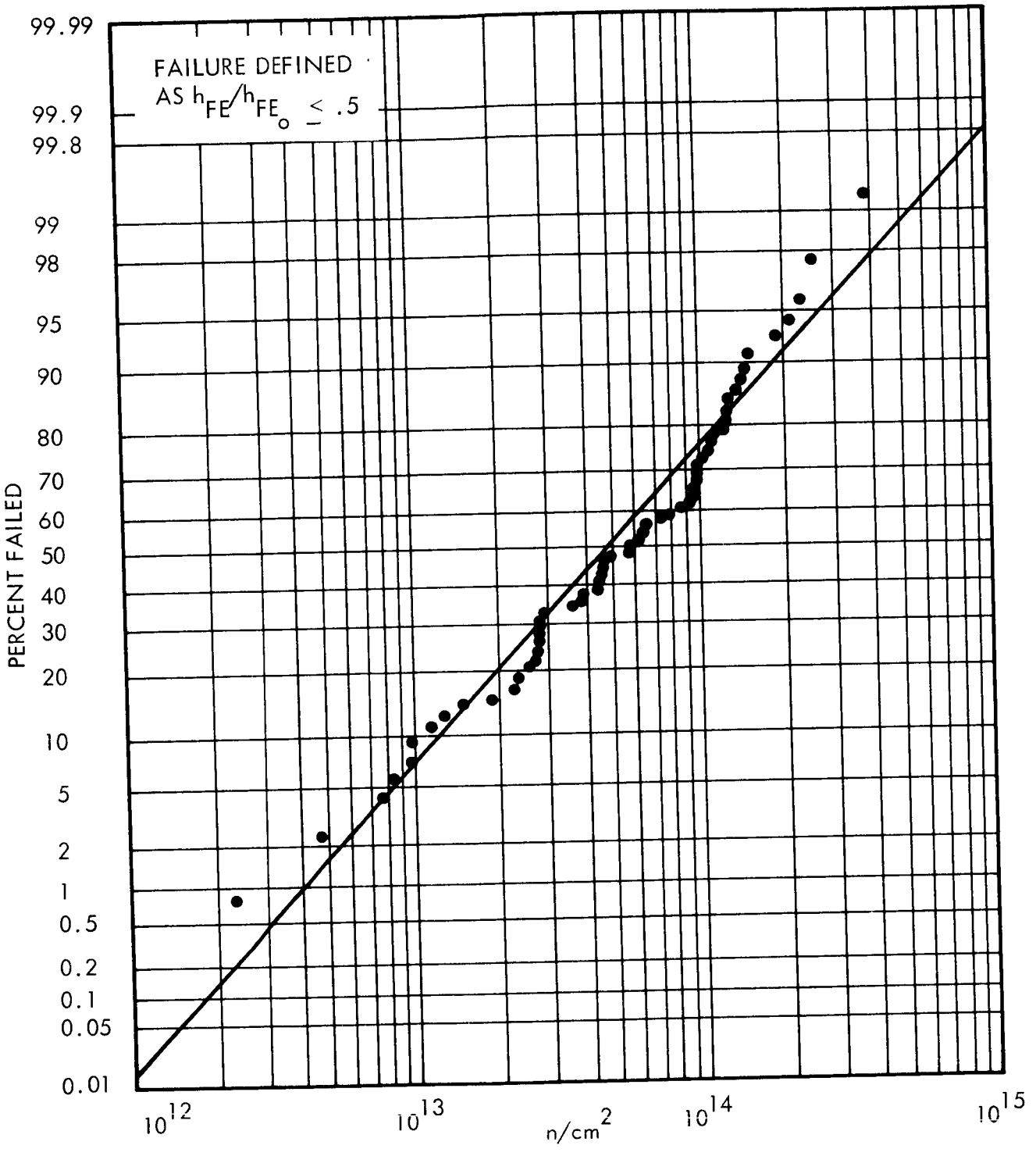

FIGURE 20 2N918 TEXAS INSTRUMENTS, 46°C, (I_C = 3 mA), PERCENT FAILED VERSUS INTEGRATED NEUTRON FLUX

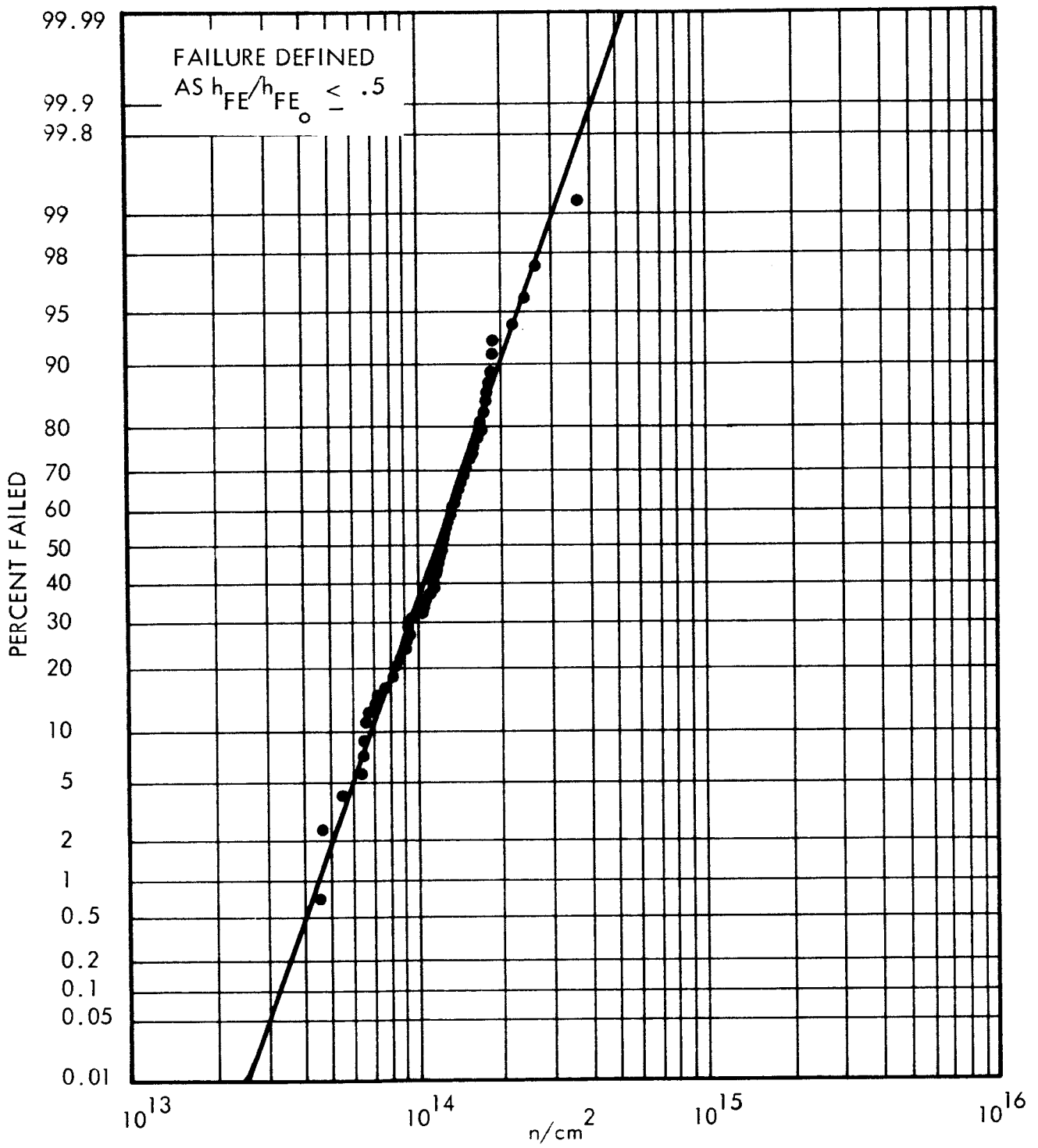

FIGURE 21 2N918 TEXAS INSTRUMENTS, 46°C, (I_C = 30 mA), PERCENT FAILED VERSUS INTEGRATED NEUTRON FLUX

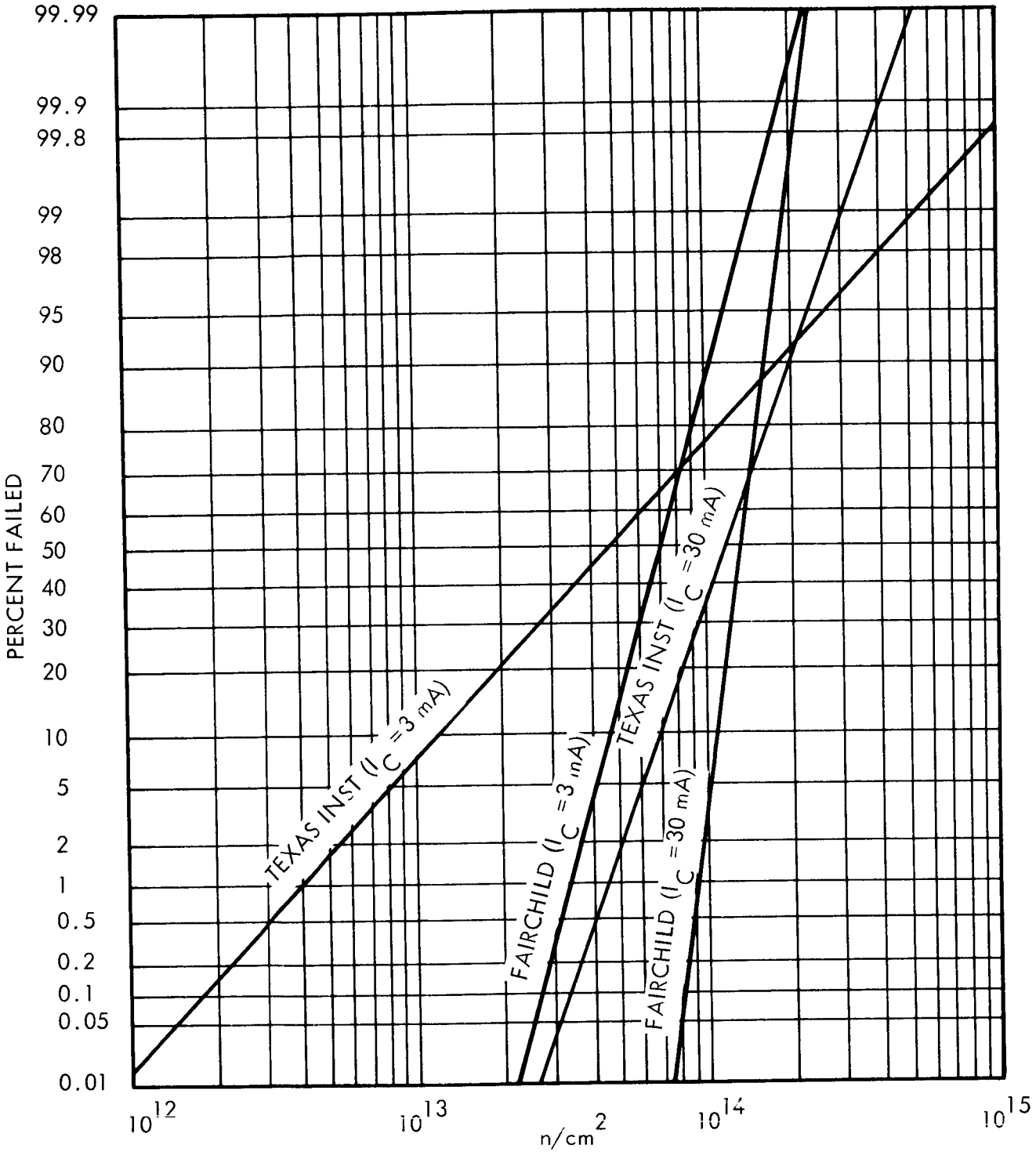

FIGURE 22 2N918, COMPARISON OF FAILURE PATTERNS FROM FIGURES 18 THROUGH 21

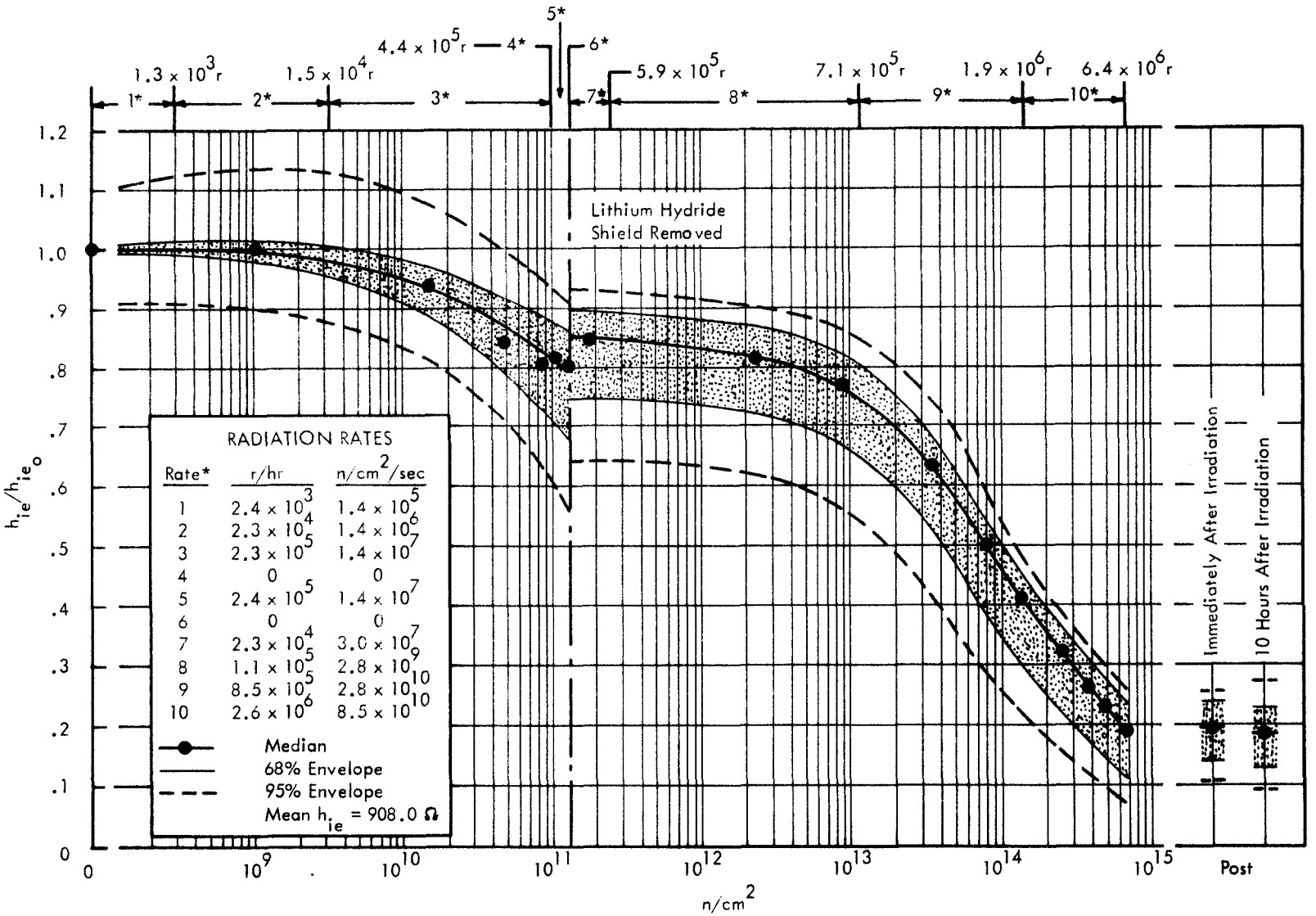

FIGURE 23 2N918 FAIRCHILD, 46° C, NORMALIZED h_{ie} VERSUS INTEGRATED NEUTRON FLUX

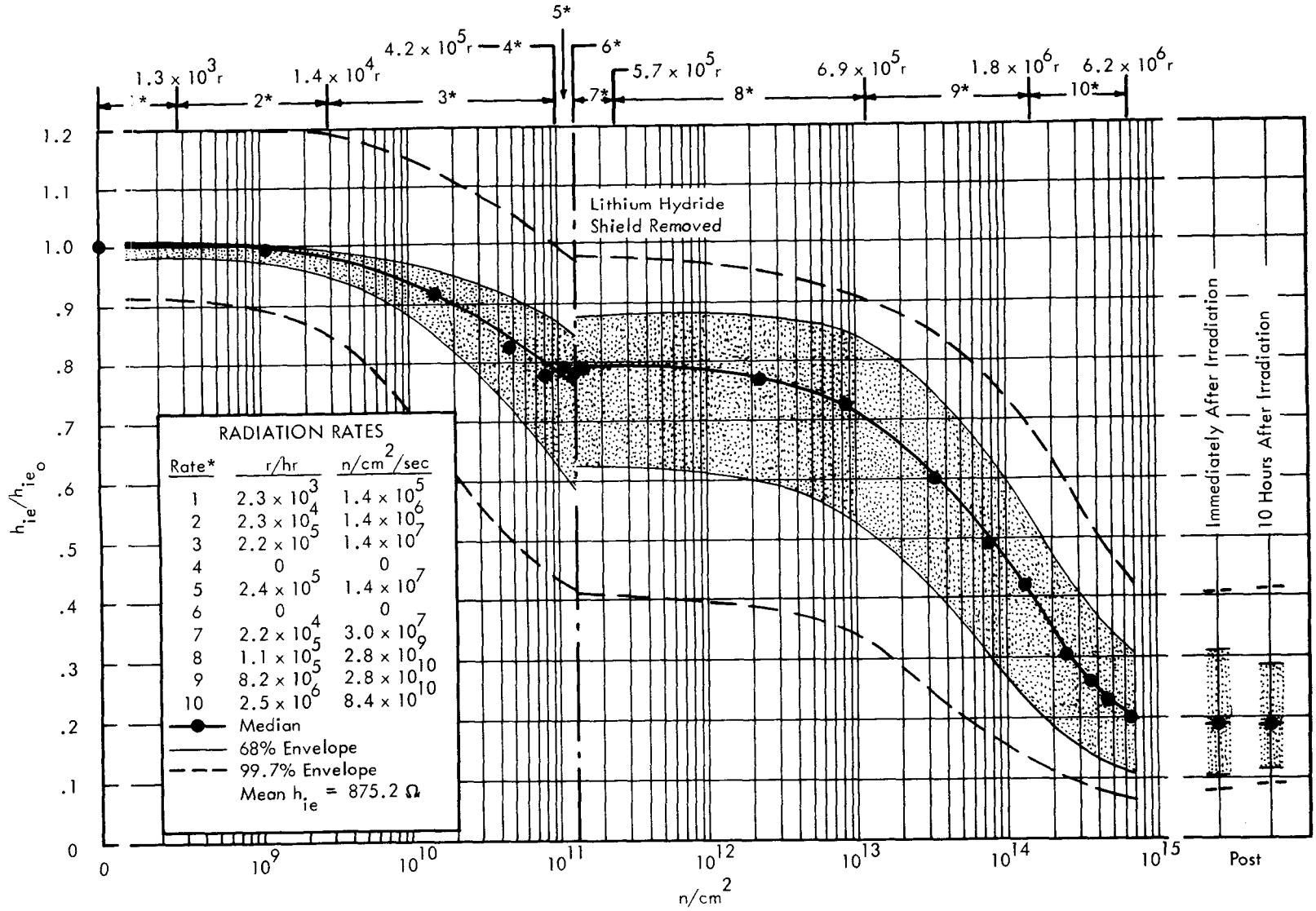

FIGURE 24 2N918 TEXAS INSTRUMENTS, 46° C, NORMALIZED h_{ie} VERSUS INTEGRATED NEUTRON FLUX

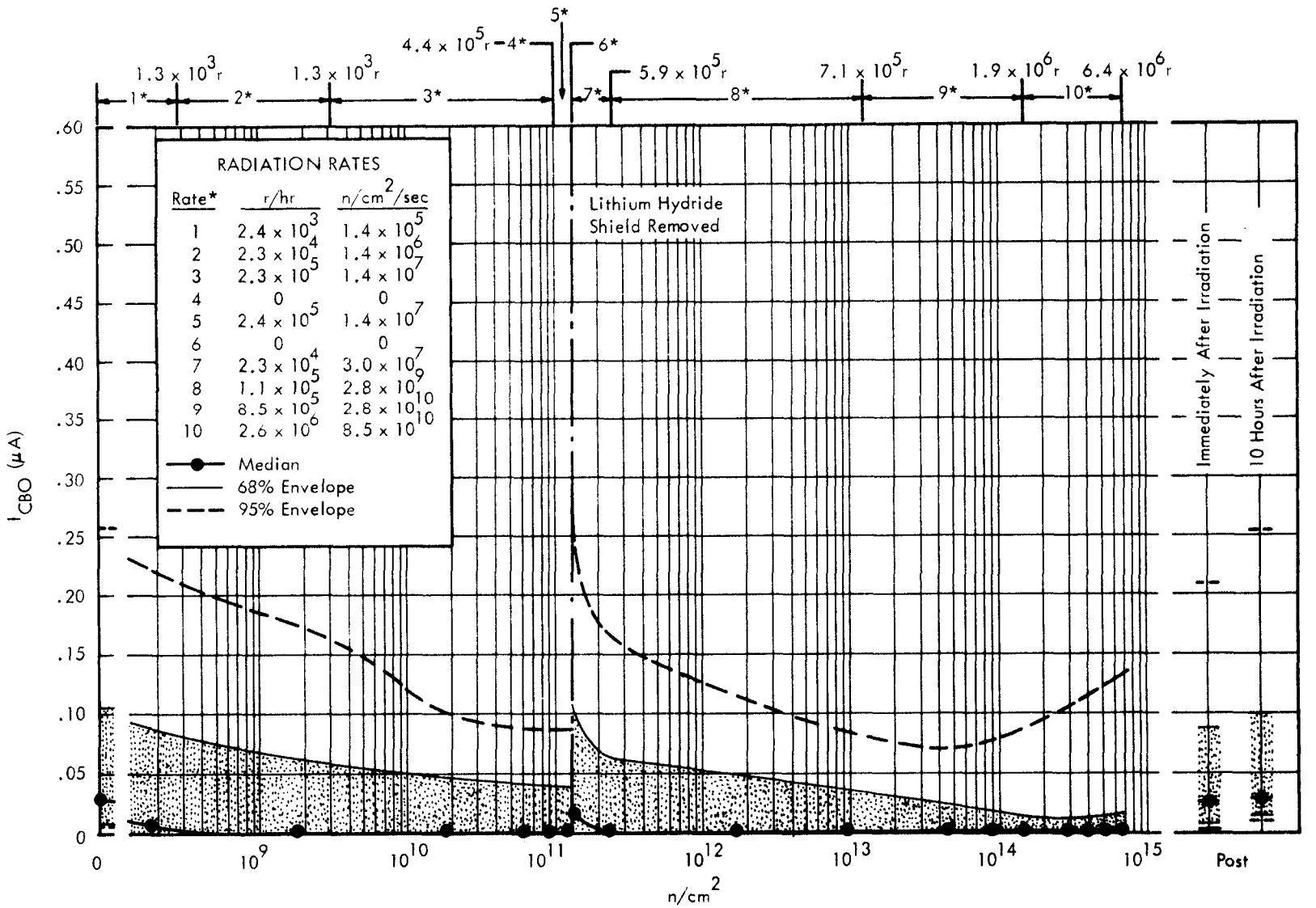

FIGURE 25 2N918 FAIRCHILD, 46° C, I_{CBO} VERSUS INTEGRATED NEUTRON FLUX

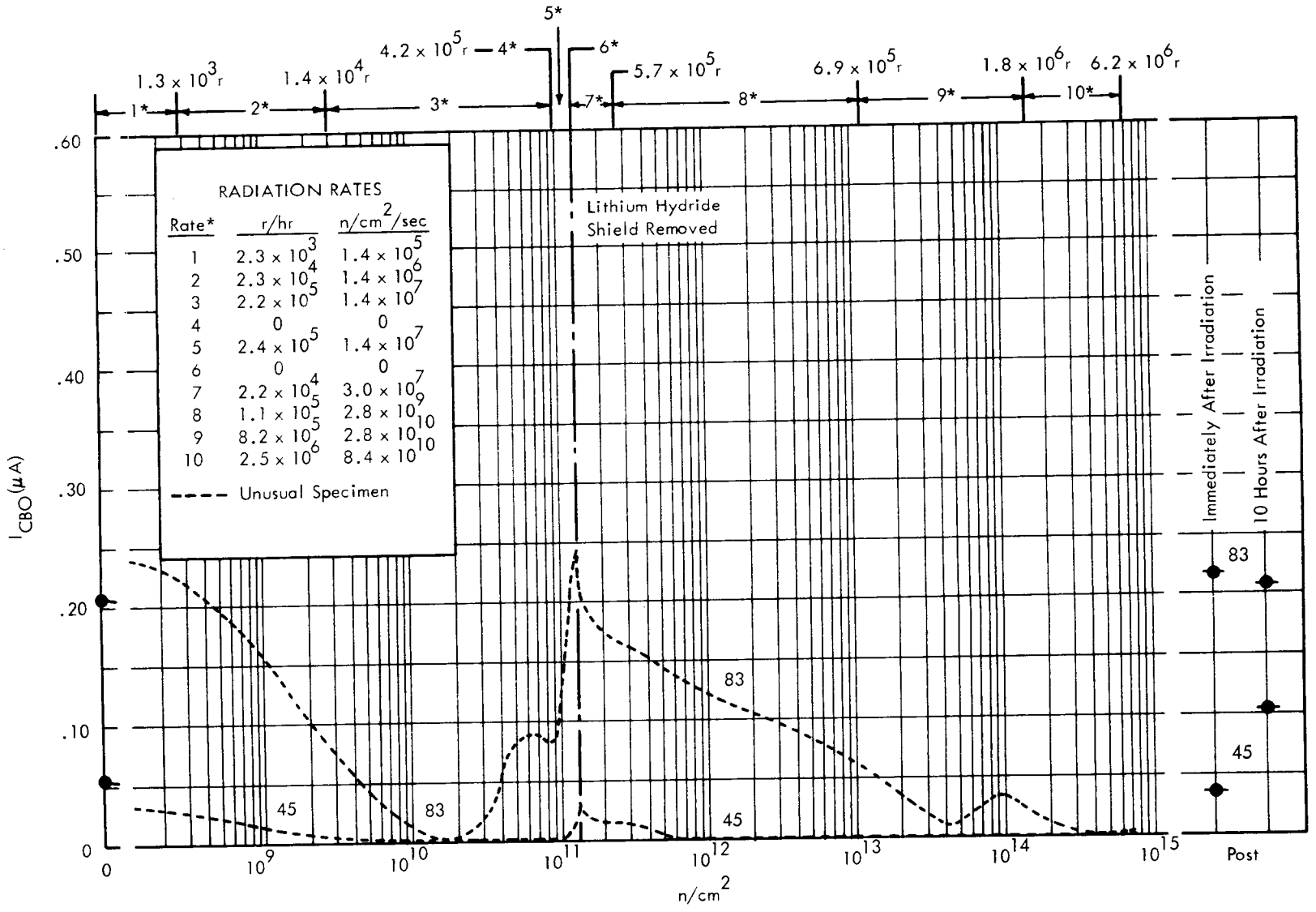

FIGURE 26 2N918 TEXAS INSTRUMENTS, 46° C, TWO "UNUSUAL" SPECIMENS, I_{CBO} VERSUS INTEGRATED NEUTRON FLUX

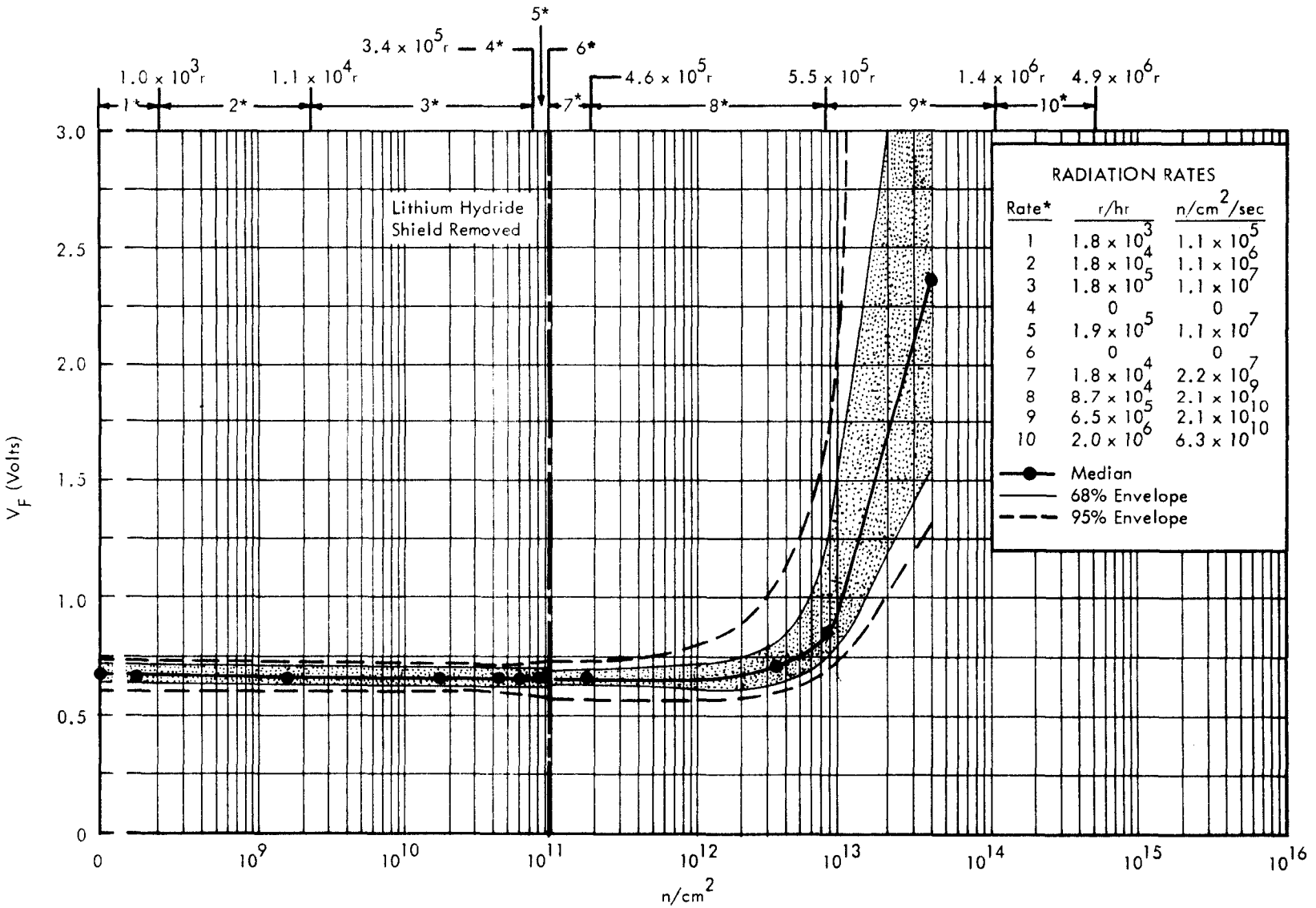

FIGURE 27 1N250 WESTINGHOUSE, 46° C, V_F (I_F .5A) VERSUS INTEGRATED NEUTRON FLUX

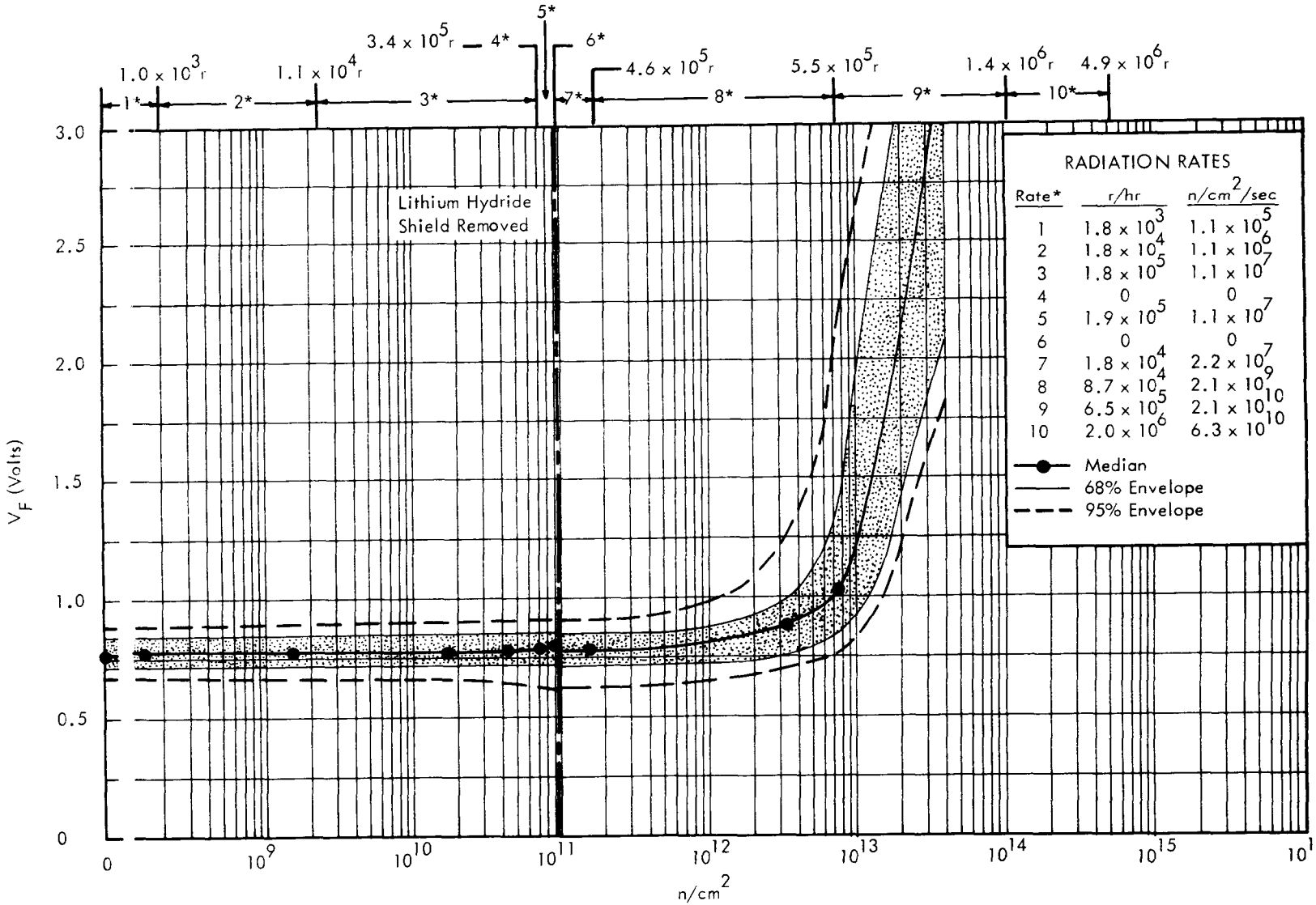

FIGURE 28 1N250 WESTINGHOUSE, 46° C, V_F (I_F = 2.5 A) VERSUS INTEGRATED NEUTRON FLUX

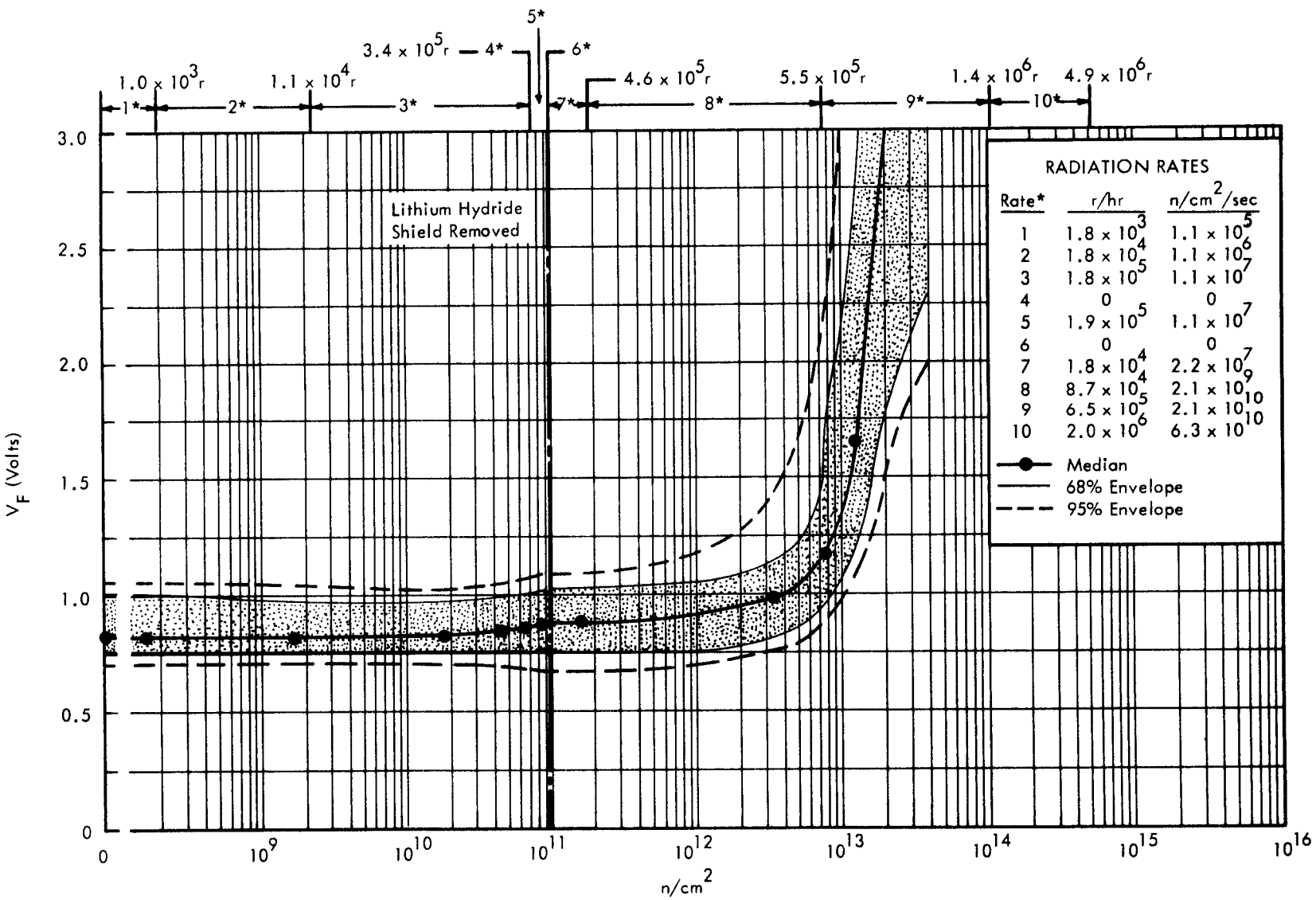

FIGURE 29 1N250 WESTINGHOUSE, 46° C, V_F (I_F = 5A) VERSUS INTEGRATED NEUTRON FLUX

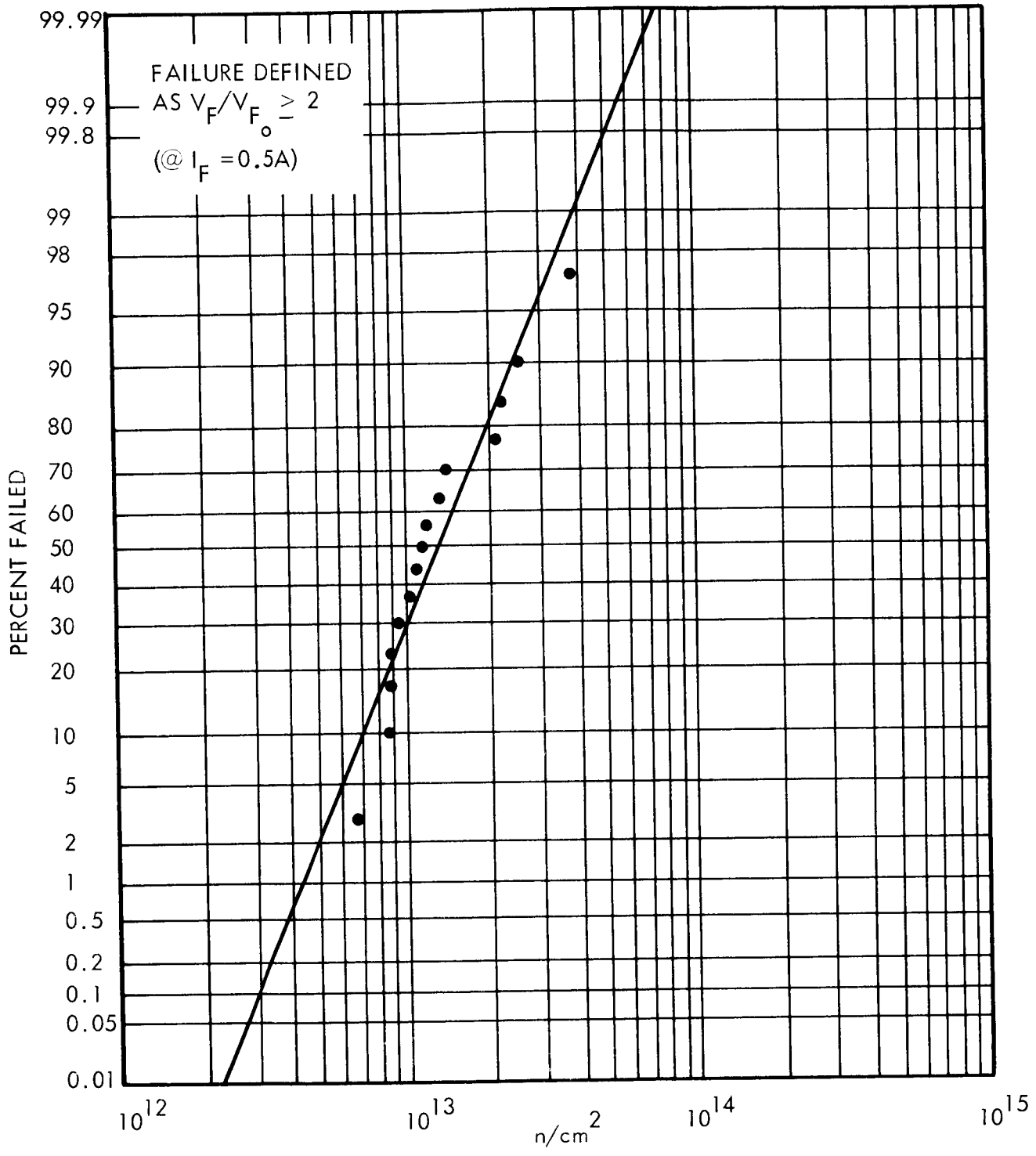

FIGURE 30 1N250 WESTINGHOUSE, 46°C, (I_F = .5A), PERCENT FAILED VERSUS INTEGRATED NEUTRON FLUX

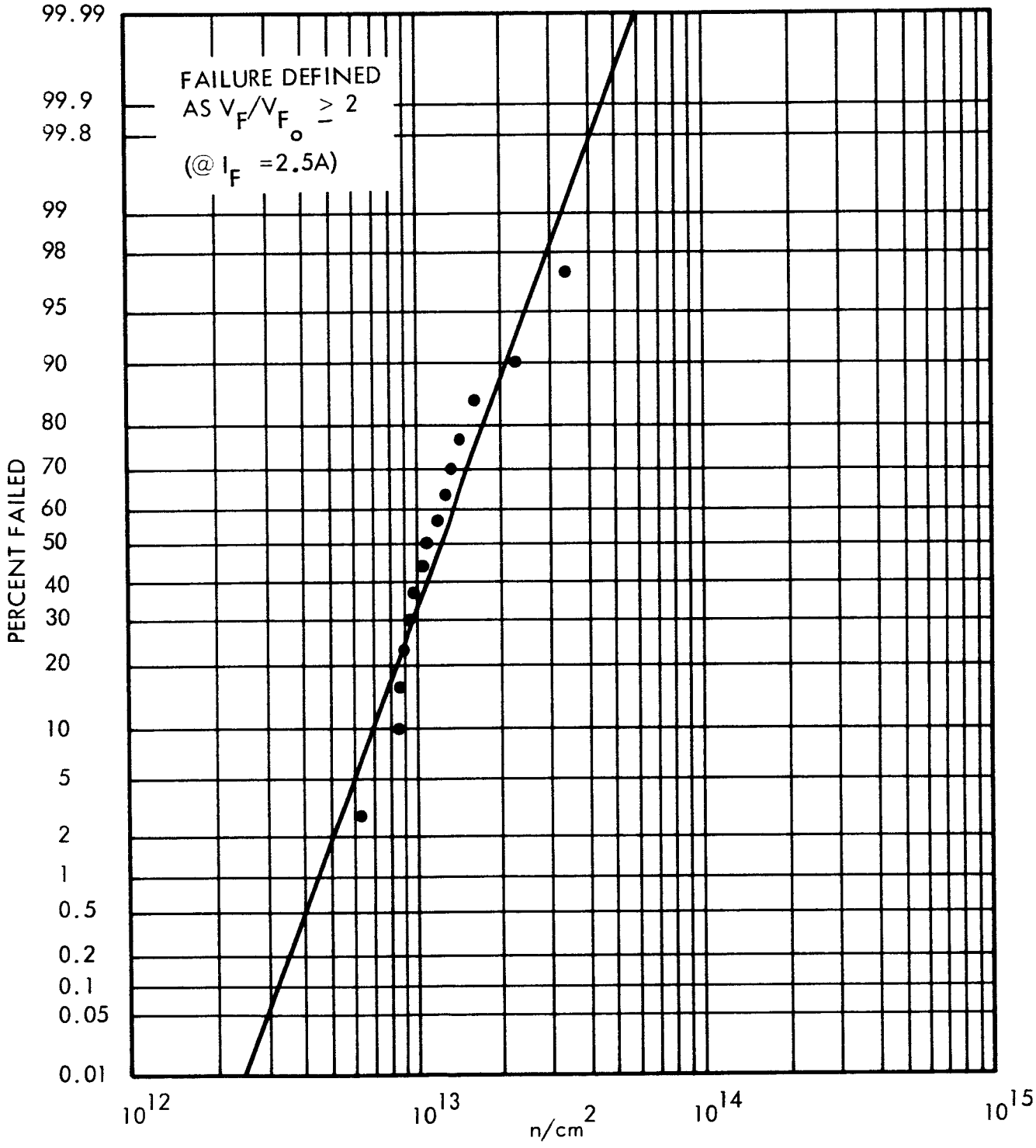

FIGURE 31 1N250 WESTINGHOUSE, 46°C, (I_F = 2.5A), PERCENT FAILED VERSUS INTEGRATED NEUTRON FLUX

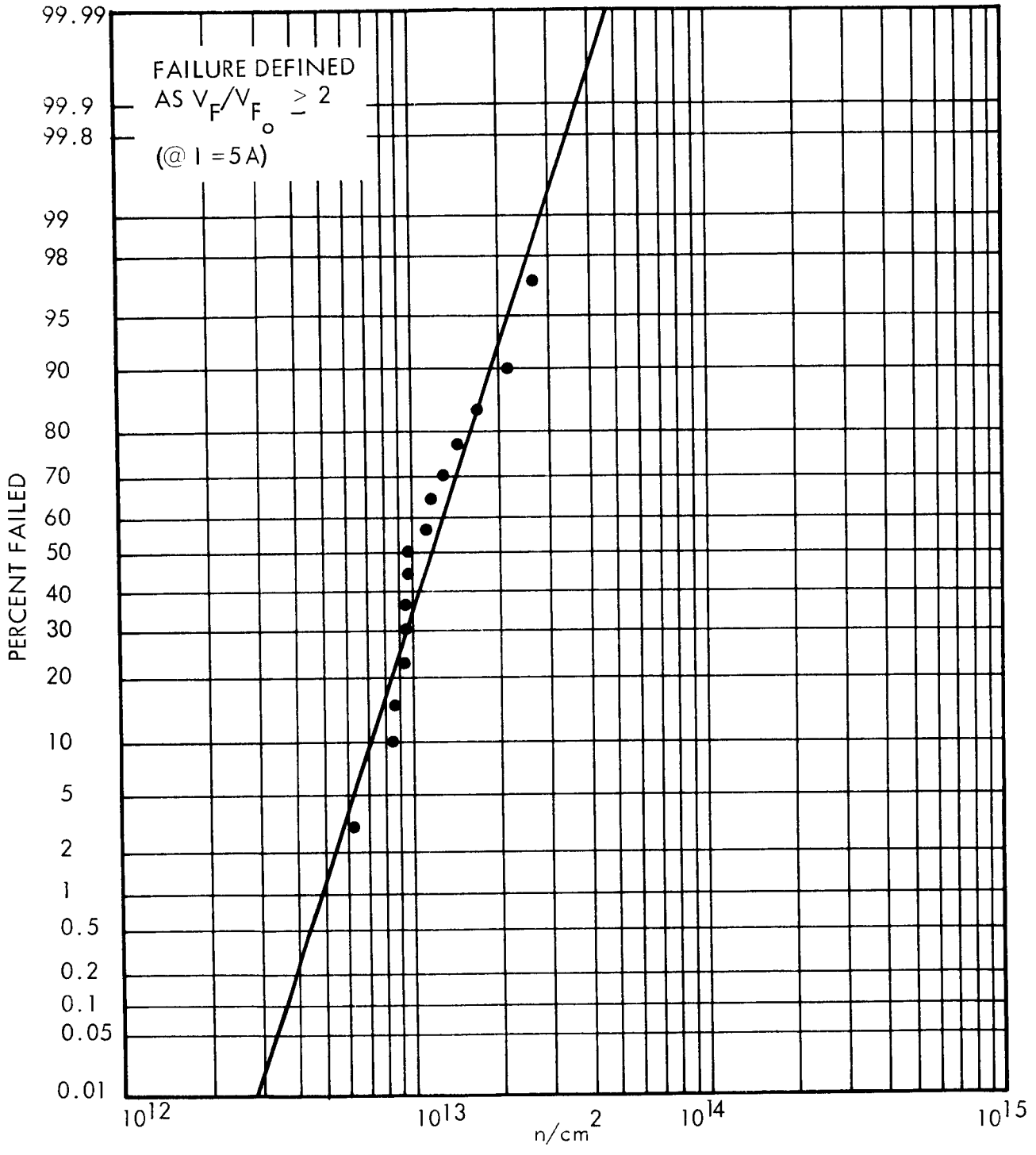

FIGURE 32 1N250 WESTINGHOUSE, 46°C, (I_F = 5A), PERCENT FAILED VERSUS INTEGRATED NEUTRON FLUX

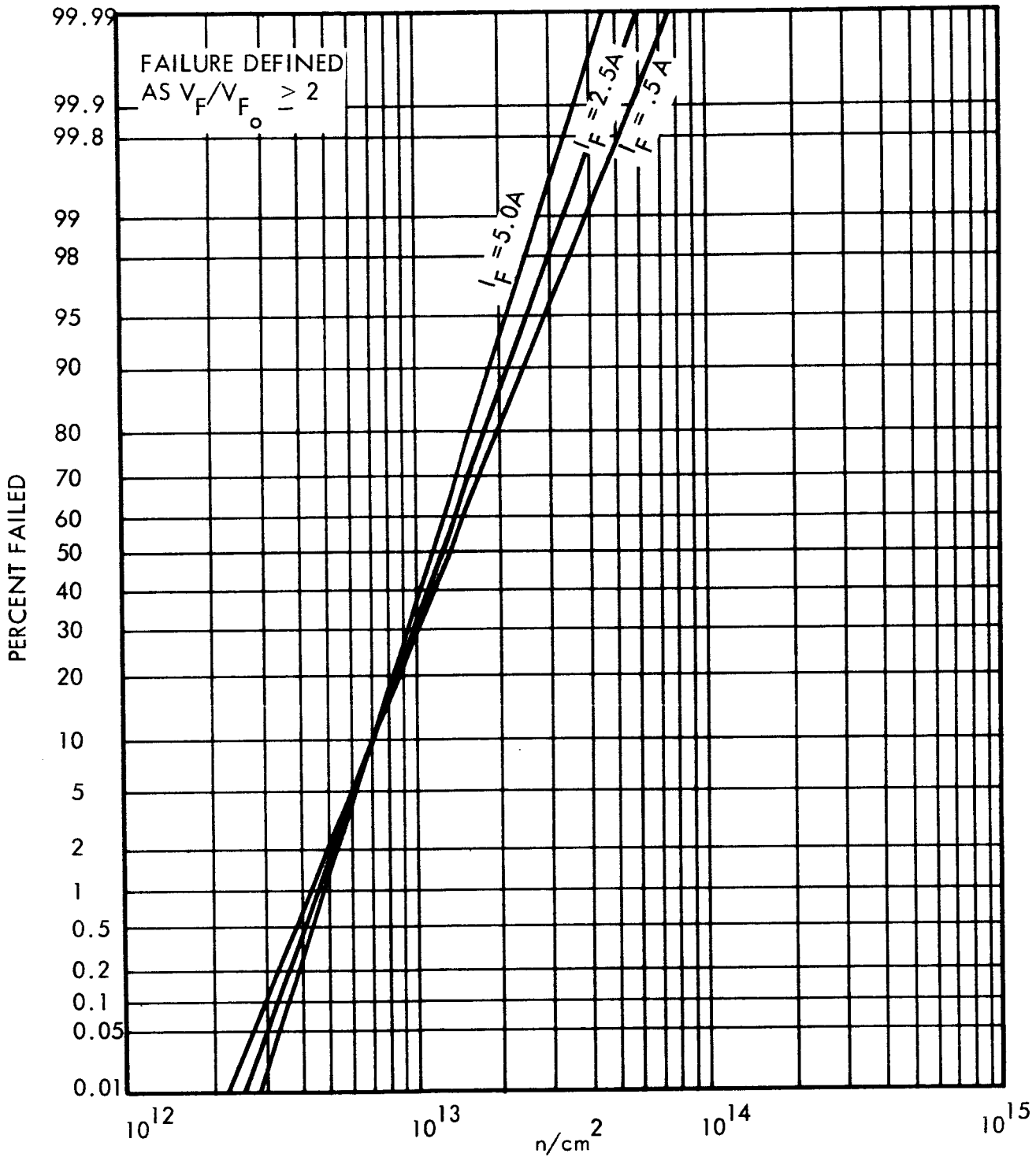

FIGURE 33 1N250 WESTINGHOUSE, COMPARISON OF FAILURE PATTERNS FROM FIGURES 30 THROUGH 32

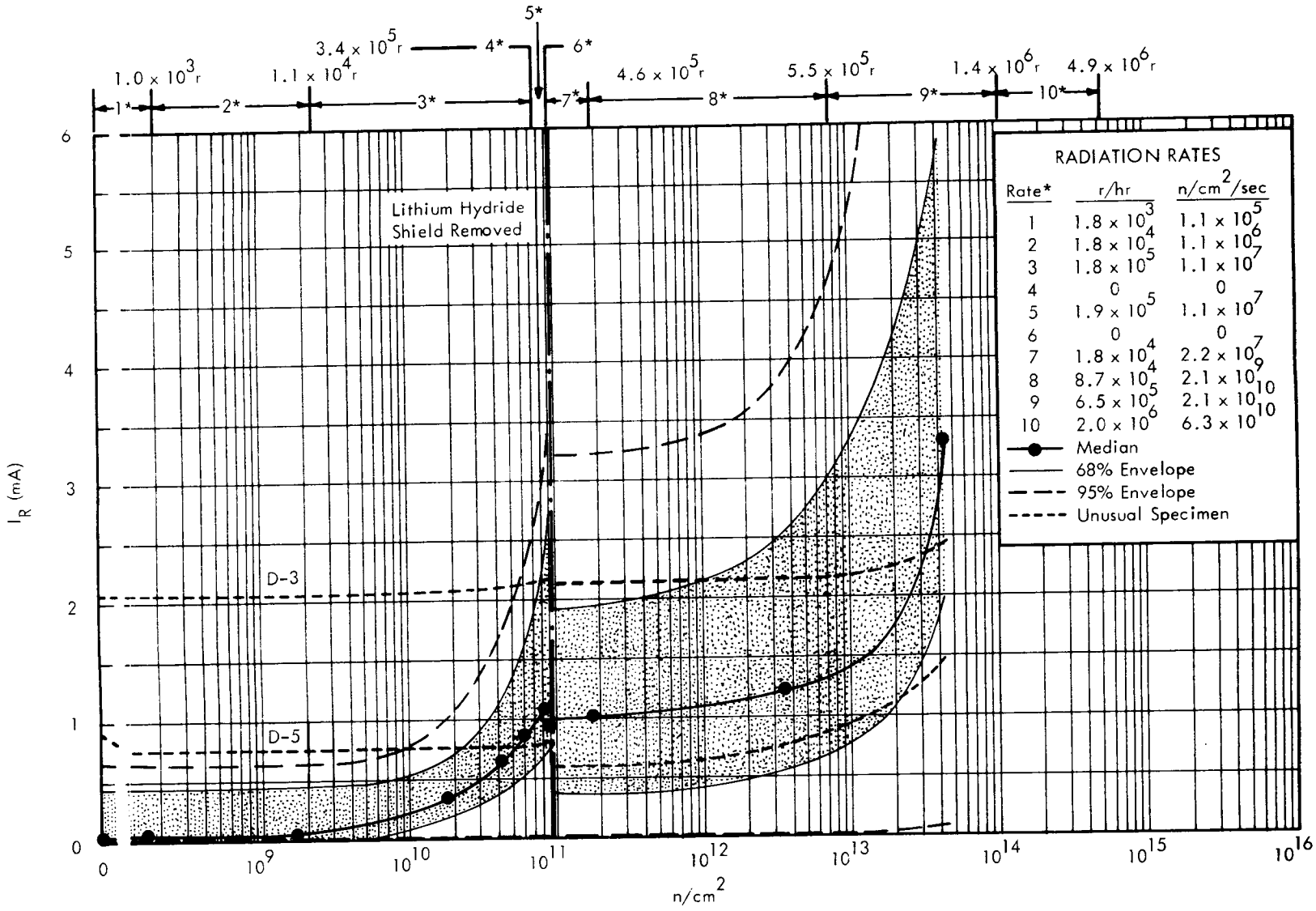

FIGURE 34 1N250 WESTINGHOUSE, 46° C, I_R (V_R = 200 V) VERSUS INTEGRATED NEUTRON FLUX

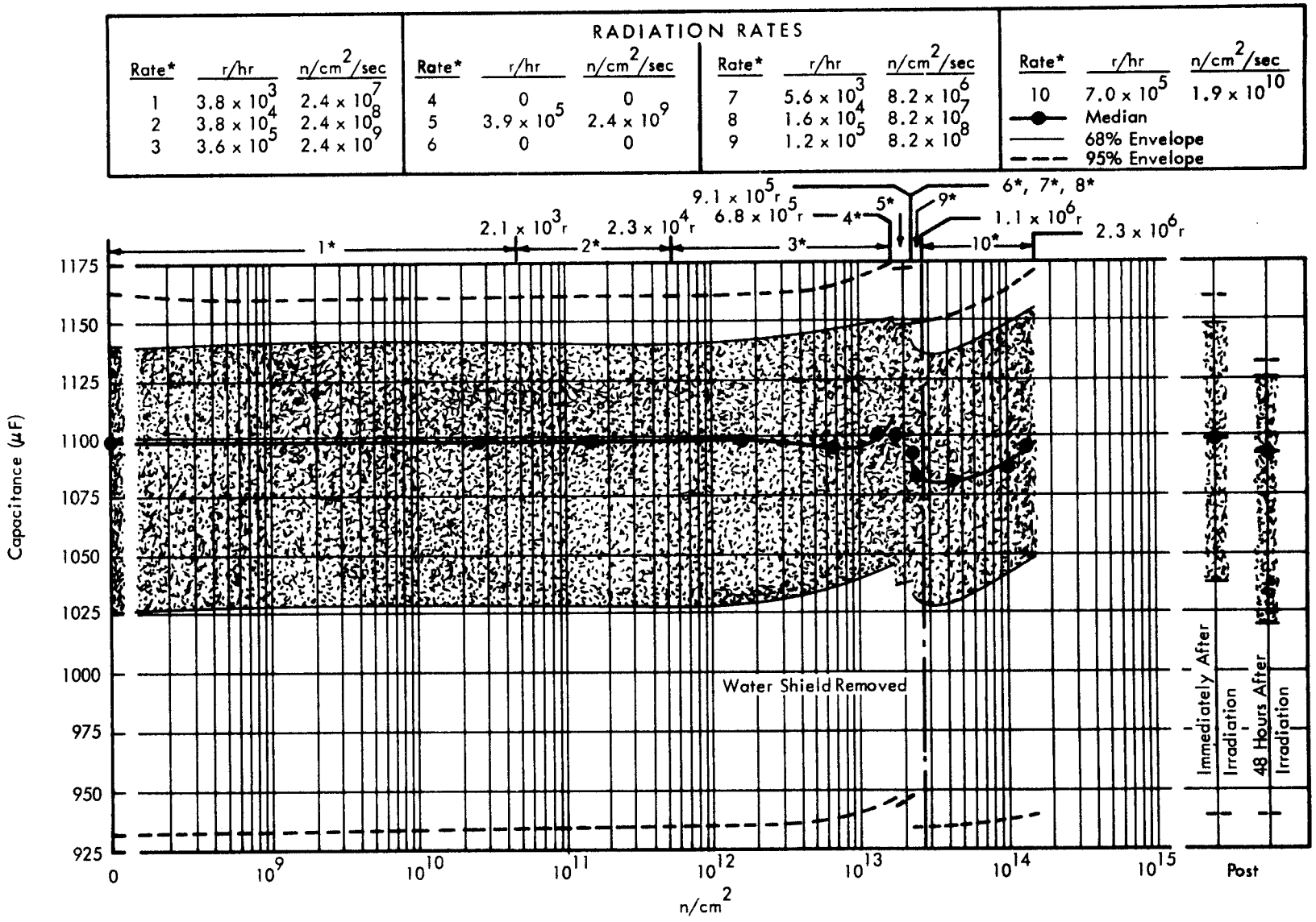

FIGURE 35 IEI 1000 μF CAPACITORS, 34 ± 6° C, CAPACITANCE VERSUS INTEGRATED NEUTRON FLUX IN VACUUM

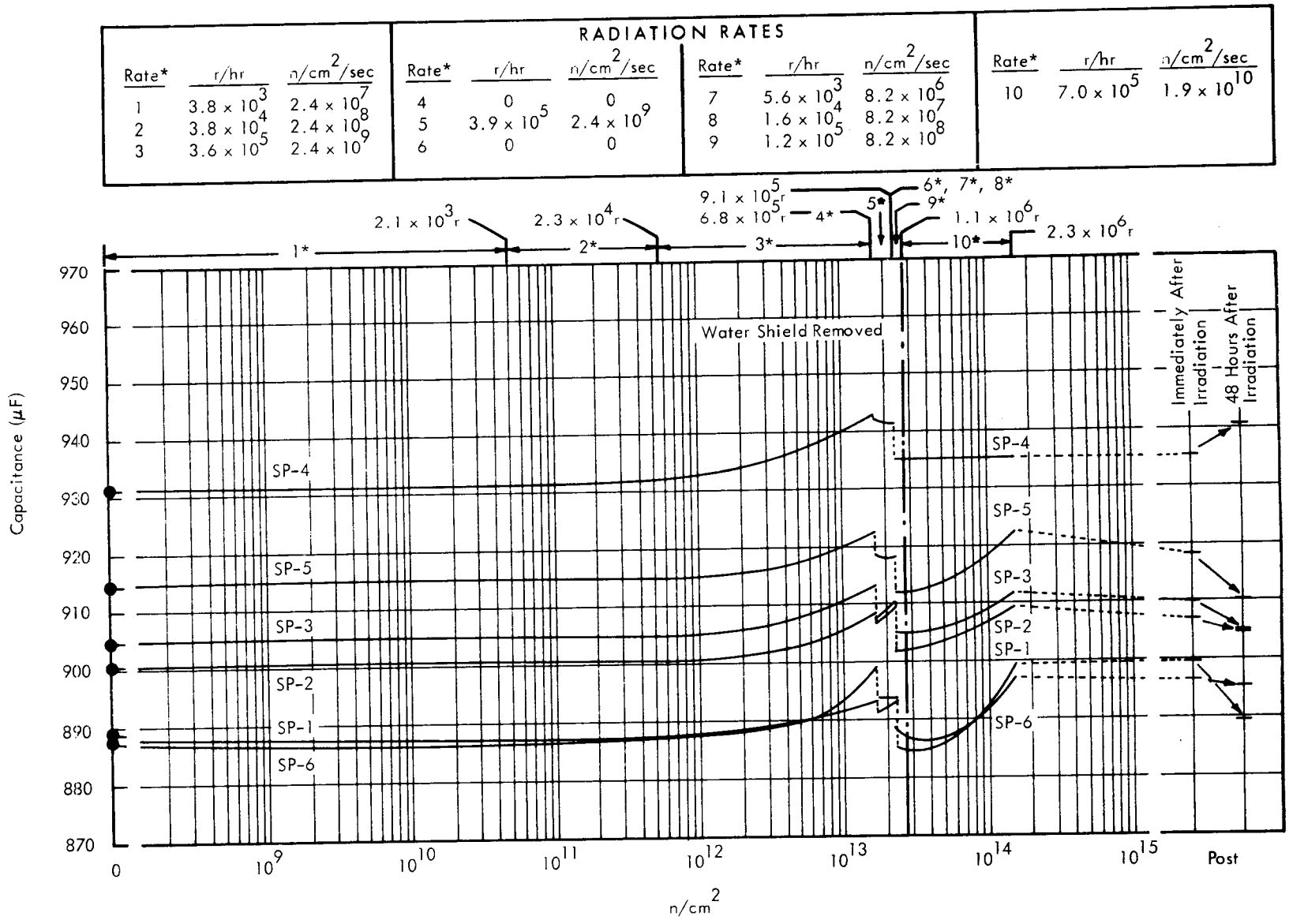

FIGURE 36 SPRAGUE 1000 μF CAPACITORS, 34 ± 6° C, CAPACITANCE VERSUS INTEGRATED NEUTRON FLUX IN VACUUM

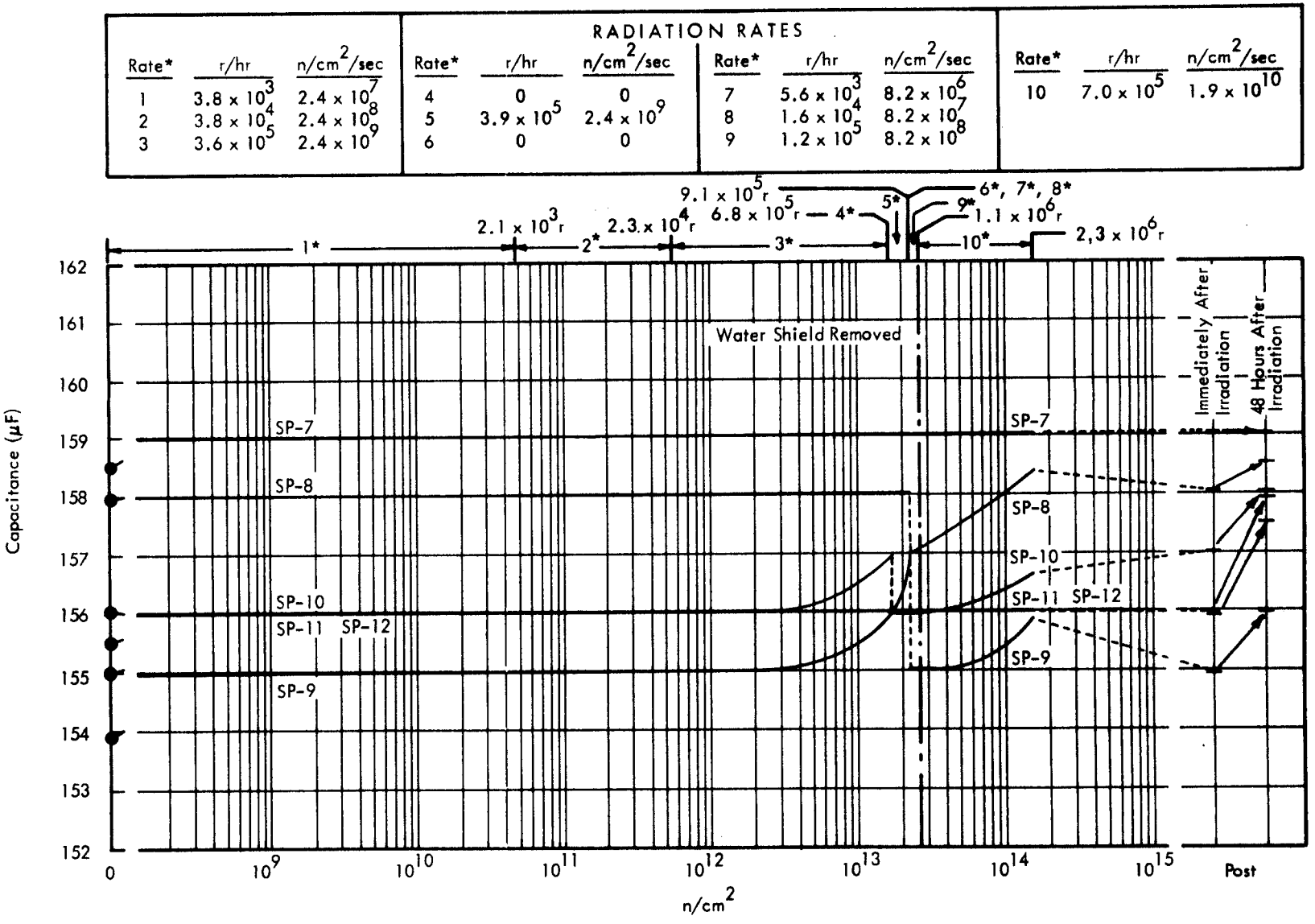

FIGURE 37 SPRAGUE 140 μF CAPACITORS, 34 ± 6° C, CAPACITANCE VERSUS INTEGRATED NEUTRON FLUX IN VACUUM

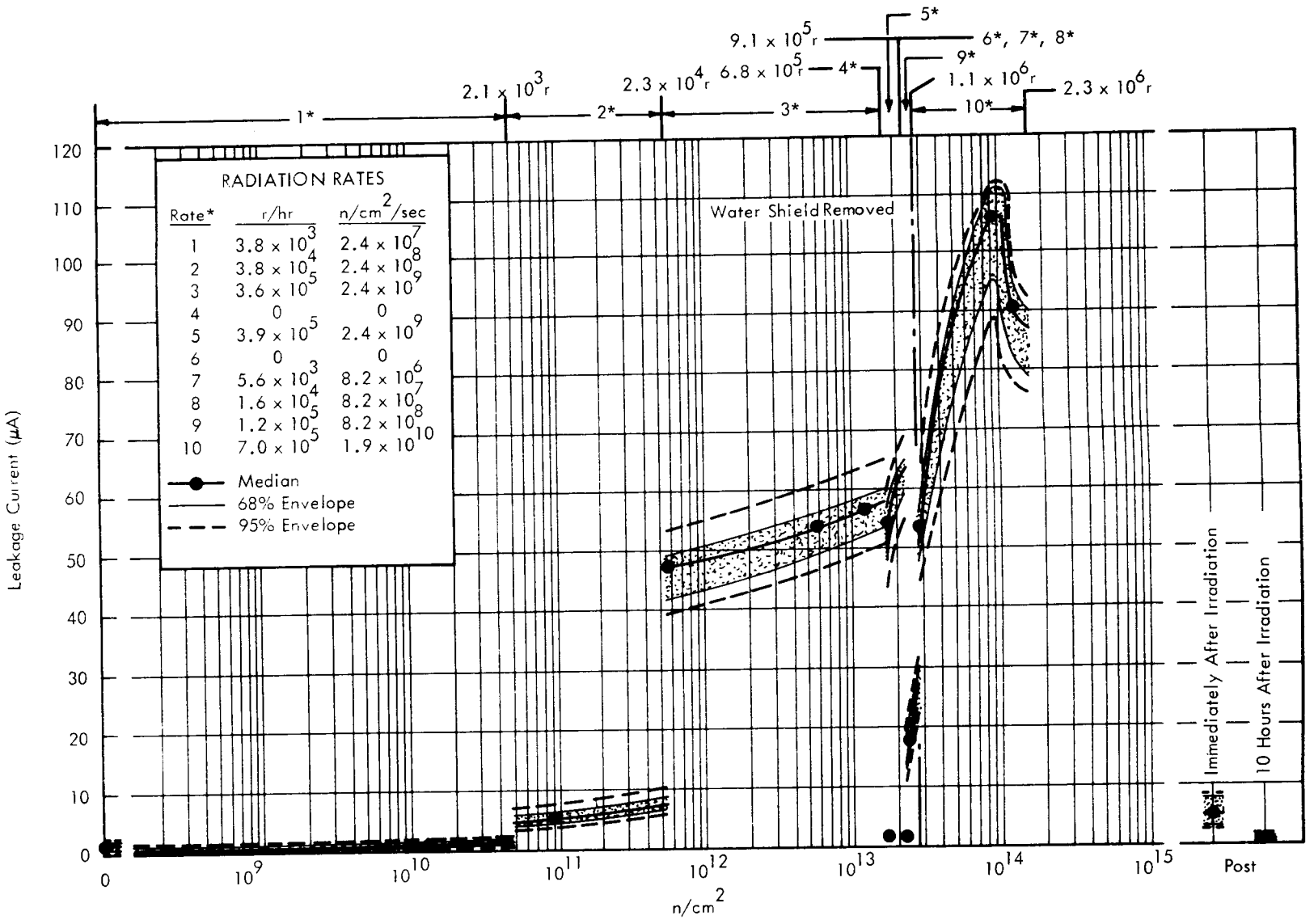

FIGURE 38 IEI 1000 μF CAPACITORS, 34 ± 6° C, LEAKAGE CURRENT VERSUS INTEGRATED NEUTRON FLUX IN VACUUM

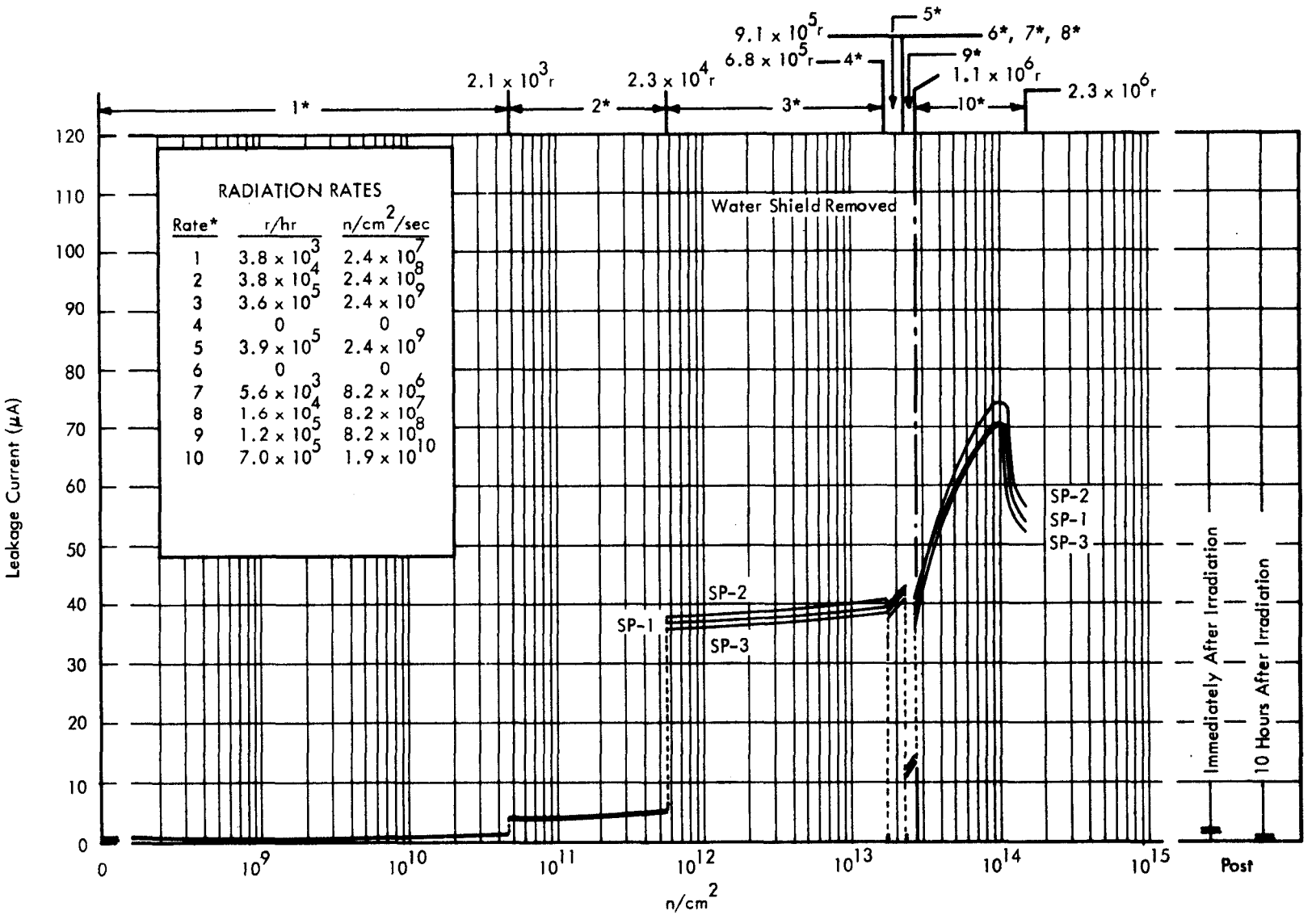

FIGURE 39 SPRAGUE 1000 μF CAPACITORS, 34 ± 6° C, LEAKAGE CURRENT VERSUS INTEGRATED NEUTRON FLUX IN VACUUM

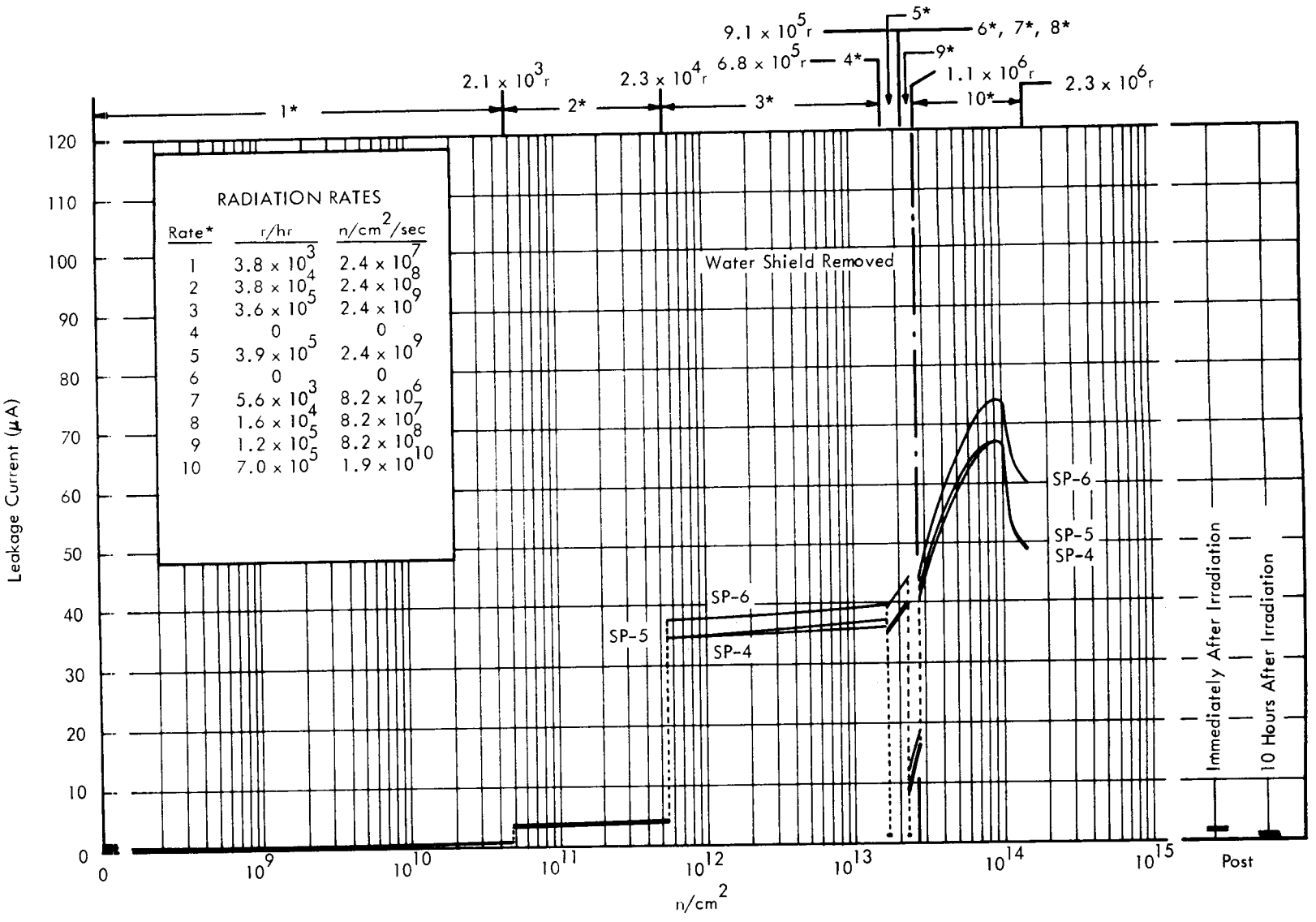

FIGURE 40 SPRAGUE 1000 μF CAPACITORS, 34 ± 6° C, LEAKAGE CURRENT VERSUS INTEGRATED NEUTRON FLUX IN VACUUM

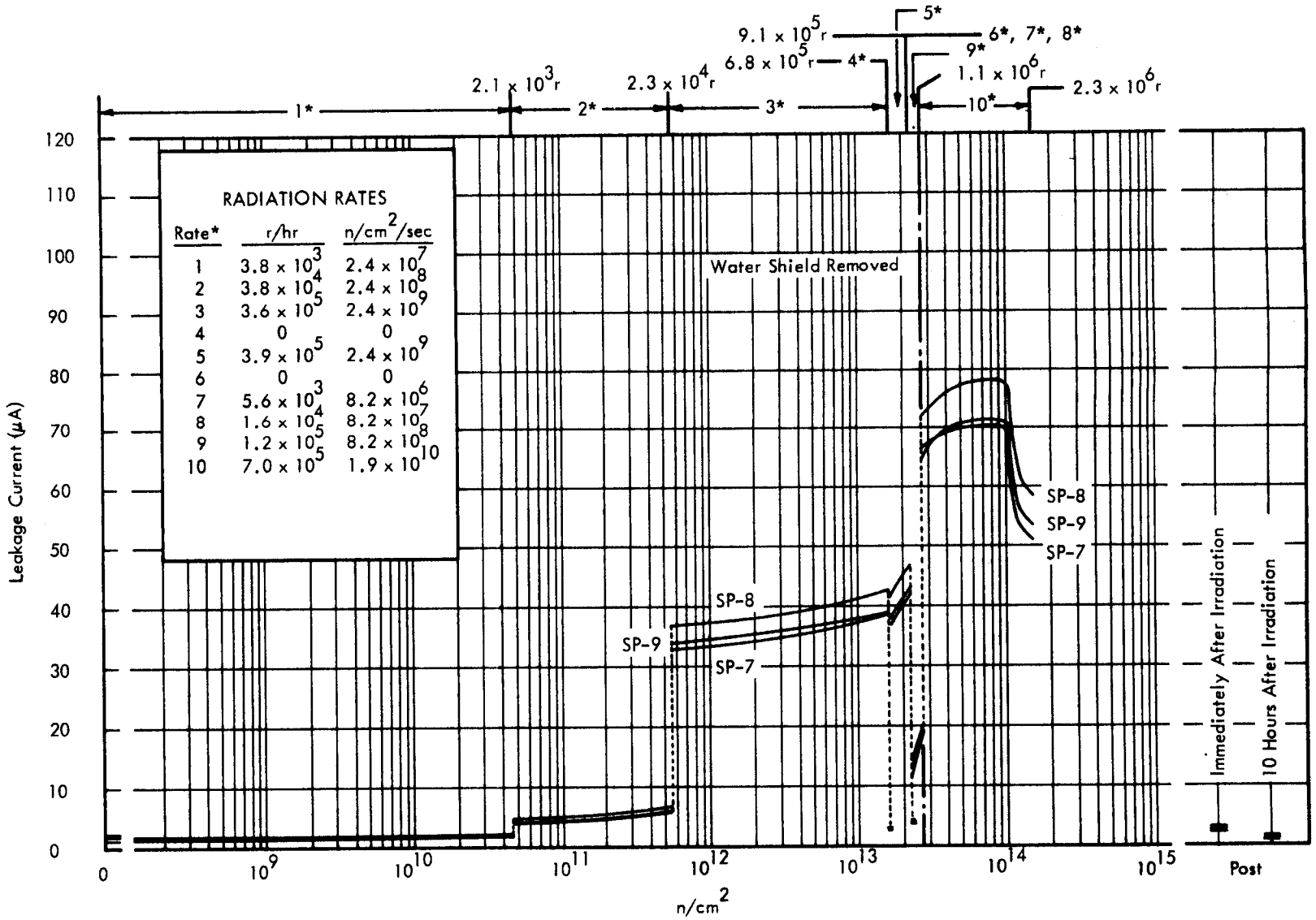

FIGURE 41 SPRAGUE 140 μF CAPACITORS, 34 ± 6° C, LEAKAGE CURRENT VERSUS INTEGRATED NEUTRON FLUX IN VACUUM

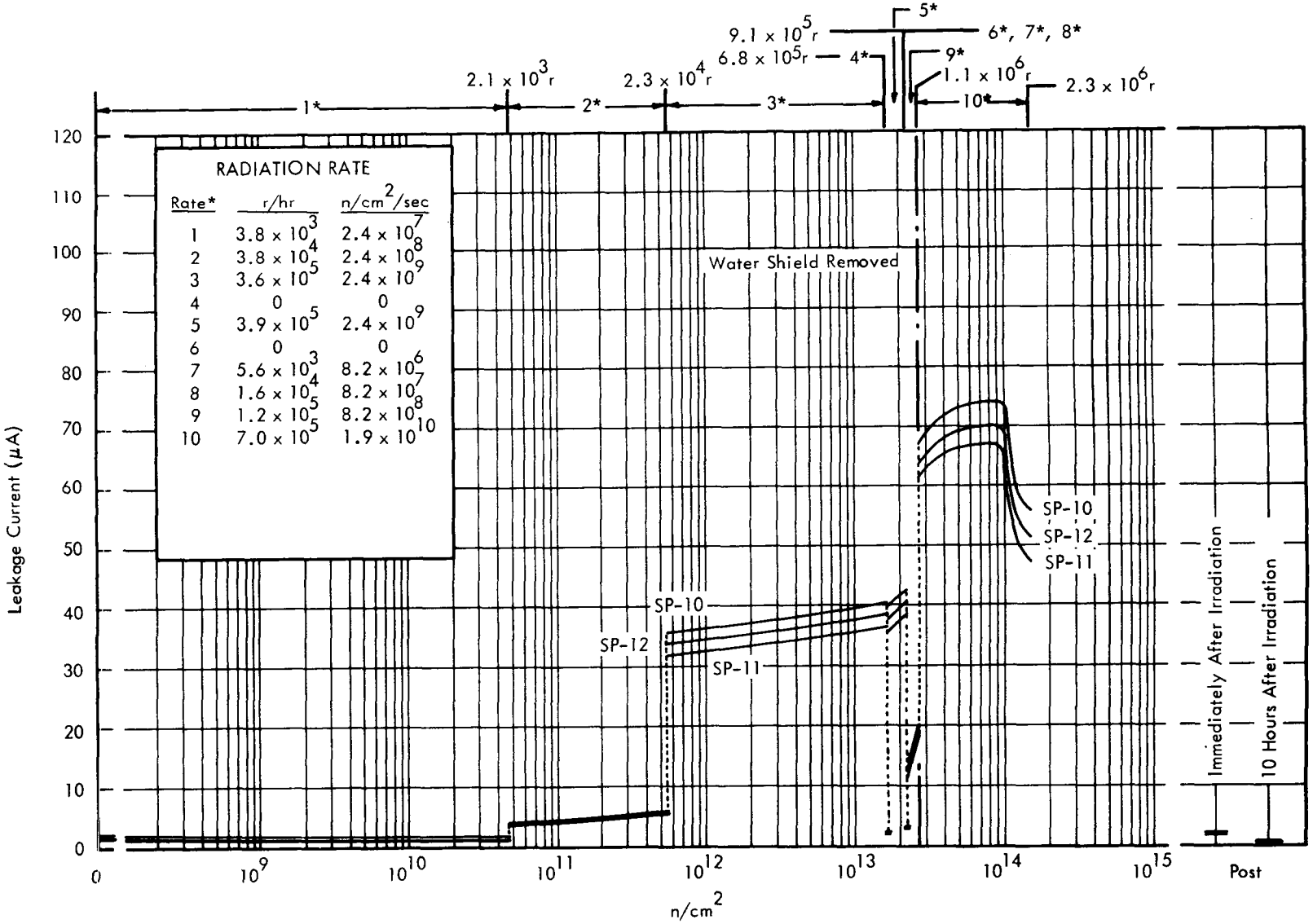

FIGURE 42 SPRAGUE 140 μF CAPACITORS, 34 ± 6° C, LEAKAGE CURRENT VERSUS INTEGRATED NEUTRON FLUX IN VACUUM